Neodymium isotopes in marginal seawater trace continental weathering inputs

Zhaojie Yu [a, b], Zehua Song [a], Xiaojie Tang [c], David J. Wilson [d], Germain Bayon [e], Yi Huang [f], Xiaoying Kang [a], Hualong Jin [a], Shiming Wan [a, b]*, Christophe Colin [c]*

[a] Key Laboratory of Marine Geology and Environment, Key Laboratory of Ocean Observation and Forecasting, Institute of Oceanology, Chinese Academy of Sciences, Qingdao 266071, China.

[b] Laboratory for Marine Geology, Qingdao Marine Science and Technology Center, Qingdao 266237, China.

[c] Université Paris-Saclay, CNRS, GEOPS, 91405, Orsay, France.

[d] London Geochemistry and Isotope Centre (LOGIC), Department of Earth Sciences, University College London, Gower Street, London, WC1E 6BT, UK.

[e] IFREMER, Marine Geoscience Unit, Plouzané, France.

[f] School of Geosciences and Info-physics, Central South University, 410083, Changsha, China.

*Corresponding author:

wanshiming@ms.qdio.ac.cn (Shiming Wan)

christophe.colin@universite-paris-saclay.fr (Christophe Colin)

Abstract

Continental weathering of silicate rocks has long been proposed as an important regulator of Earth's climate over geological timescales. However, whether silicate weathering fluxes have increased, decreased, or remained unchanged during the Cenozoic, and across glacial-interglacial cycles, remains under debate. A major source of uncertainty stems from the multiple controls on weathering proxies and a lack of consistency between existing records. Seawater neodymium (Nd) isotopes have been extensively used to trace the mixing and evolution of water masses in the open ocean. Here, an emerging application of seawater Nd isotopes to trace continental weathering inputs based on marine sediment records from marginal settings is reviewed and applied to the northern

Indian Ocean. Seawater Nd isotope observations and reconstructions in the Bay of Bengal spanning a range of timescales (modern – millennial – orbital – tectonic) reveal a strong influence of South Asian continental weathering inputs, which may be related to drivers such as Himalayan tectonic uplift and monsoon precipitation. The long-term evolution of seawater Nd isotopes in the Bay of Bengal has the potential to trace the evolving Himalayan weathering inputs since the Oligocene, and to reveal the links between tectonics, climate, and weathering, while there were also weathering changes on orbital timescales in the Pleistocene. While demonstrating the strong potential of marginal seawater Nd isotopes in tracing past continental weathering inputs, more research on particle-seawater interaction processes and on the quantitative relationship between Nd isotopes and weathering inputs is still needed.

Key words: Seawater Nd isotopes, Continental weathering, Carbon cycle, Bay of Bengal, Himalayan uplift

1. Introduction

Chemical weathering is the process of rock and mineral decomposition under the influence of water, atmospheric gases, climate, and other factors such as vegetation and biology. Due to its physical and chemical effects, weathering plays an important role in the interactions between the atmosphere, the hydrosphere, the lithosphere, and the biosphere. On million-year timescales, the consumption of atmospheric CO_2 by the chemical weathering of silicate rocks and its ultimate sequestration in marine carbonate rocks ($CaSiO_3 + CO_2 = CaCO_3 + SiO_2$) is considered an important process for driving climate change and maintaining the relative climate stability and hence habitability of the Earth (Berner et al., 1983; Walker et al., 1981). However, recent field observations suggest that chemical weathering in high mountain and glaciated environments could instead act as

48 a net source of atmospheric CO_2, due to the oxidation of fossil organic matter and sulfide minerals
49 (Bufe et al., 2024; Horan et al., 2017; Liu et al., 2023; Liu et al., 2025; Torres et al., 2016; Torres et
50 al., 2014; Zondervan et al., 2023), indicating that continental weathering is not always a net carbon
51 sink. In parallel, silicate chemical weathering has been found to react rapidly to climatic and
52 environmental changes, producing feedbacks on climate even on orbital or millennial timescales, as
53 inferred from modern observations (Arnscheidt and Rothman, 2022; Beaulieu et al., 2012; Colbourn
54 et al., 2015; Gislason et al., 2009), as well as from mineralogical and geochemical records (Bastian
55 et al., 2017; Dosseto et al., 2015; Miriyala et al., 2017).

56 Reconstructing the past evolution of chemical weathering fluxes is key to reveal the role of
57 weathering in the carbon cycle, as such estimates can be used to directly assess the amount of
58 atmospheric CO_2 consumed through weathering e. The chemical weathering flux refers to the
59 dissolved elemental budget released from weathered rock per unit time in a given system, such as
60 from a river catchment, and is positively correlated with the chemical weathering rate. There are
61 two main weathering regimes in the natural environment: transport-limited weathering (occurring
62 in lowlands dominated by thick soils and low erosion rates, such as tropical floodplains), and
63 kinetically-limited weathering (occurring in highlands dominated by high erosion rates, such as in
64 Southeast Asian islands) (West et al., 2005). In lowlands, chemical weathering fluxes are limited by
65 the supply of fresh material, and hence are directly linked to erosion rates, while they are partly
66 decoupled in high-elevation environments, where the link between erosion rates and chemical
67 weathering fluxes becomes strongly non-linear (Bayon et al., 2020; Bouchez et al., 2012; West,
68 2012).

69 To date, reconstructing past silicate chemical weathering fluxes, at catchment, regional, or

global scales, is still a challenge. Specifically, most of the mineralogical, elemental, and isotopic proxies measured on terrigenous silicate detritus can only indicate the degree of chemical weathering of the sediment (i.e. weathering intensity), but cannot reflect changes in the chemical weathering flux (Perri, 2020). Converting such information into quantified silicate weathering fluxes is possible, but involves relatively large uncertainties (Clift et al., 2024). Therefore, researchers have instead used proxy records of the isotopic composition of seawater to indirectly reconstruct past chemical weathering inputs (Vance et al., 2009). The basic principle behind this approach is that the isotopic composition of dissolved elements in seawater is the result of mixing between the continental weathering inputs and the background sources to seawater, such as mid-ocean ridge hydrothermal inputs (for elements like Sr or Li) or benthic fluxes linked to early diagenesis in the marine sediment (for reactive elements such as the rare earth elements) (Hodell et al., 1990; Misra and Froelich, 2012). Continental chemical weathering fluxes at ocean margins include both dissolved riverine inputs and the dissolution/release from terrigenous particles supplied by rivers and dust to seawater (van de Flierdt et al., 2016). In this context, the isotopic composition of reactive elements in seawater, as recorded in archives such as marine biogenic material (e.g. foraminifera, diatoms) or authigenic mineral phases (e.g. iron and manganese oxyhydroxides) extracted from marine sediment, can be used to generate records of past continental weathering changes (Lein, 2004; Tachikawa et al., 2014).

2. Seawater isotope proxies tracing continental weathering inputs

Several different seawater isotope proxies have commonly been used to reconstruct global continental weathering inputs over a range of timescales, including strontium (Sr), osmium (Os), lithium (Li), and beryllium (Be) isotopes. However, the controls on each of these proxies vary, and

92 the evidence they provide on continental weathering inputs can be inconsistent. For example,
93 seawater Sr and Li isotope records have historically been interpreted as reflecting an increase in
94 continental chemical weathering inputs through the Cenozoic (Misra and Froelich, 2012; Raymo
95 and Ruddiman, 1992), although hydrothermal inputs have been proposed recently (Weldeghebriel
96 and Lowenstein, 2023). Additionally, seawater Be isotope records have been interpreted as
97 reflecting relatively stable global denudation and related weathering fluxes during both the
98 Cenozoic (Willenbring and von Blanckenburg, 2010) and the Quaternary period (von Blanckenburg
99 et al., 2015). However, these findings were challenged in recent studies (Deng et al., 2023; Li et al.,
100 2021), illustrating the complexity of interpreting sedimentary records of seawater chemistry as
101 archives of past continental chemical weathering fluxes. Below, the principles and some key
102 findings from the above isotope tracers are briefly reviewed.
103 Seawater radiogenic Sr isotopes mainly reflect a balance between two major sources:
104 continental weathering inputs with radiogenic Sr isotopes ($^{87}Sr/^{86}Sr$ ~ 0.7111) and submarine
105 hydrothermal inputs with unradiogenic Sr isotopes ($^{87}Sr/^{86}Sr$ ~ 0.70305) (Edmond, 1992; Peucker-
106 Ehrenbrink et al., 2010). Assuming that the rate of seafloor spreading and the Sr isotope composition
107 of hydrothermal inputs remained unchanged (Dalton et al., 2022; Edmond, 1992), the increase in
108 seawater Sr isotopes during the Cenozoic was interpreted to indicate an increase in continental
109 silicate weathering fluxes (Edmond, 1992; Raymo and Ruddiman, 1992; Yang et al., 2023). This
110 explanation was broadly consistent with the concept that collision and uplift of the Himalaya during
111 the Cenozoic (the "uplift-weathering" hypothesis) had led to an intensification of the South Asian
112 monsoon and associated chemical weathering of silicate rocks, thereby leading to atmospheric CO_2
113 drawdown (Raymo and Ruddiman, 1992). However, there are other potential explanations for the

114 increase in seawater Sr isotopes during the Cenozoic, including: (1) a source control due to the
115 weathering of Himalayan metamorphosed carbonate rocks with unusually high $^{87}Sr/^{86}Sr$ ratios
116 (Blum, 1997; Quade et al., 1997); (2) changes in the rate of seafloor spreading and associated
117 hydrothermal input fluxes (Weldeghebriel and Lowenstein, 2023); and (3) temperature-dependent
118 changes in the Sr fluxes from low-temperature alteration of ocean crust (Coogan and Dosso, 2015).
119 Similar to Sr isotopes, seawater Os isotope records for the Cenozoic have also been interpreted
120 to reflect increases in continental weathering inputs. There are three main sources of Os to seawater:
121 terrestrial weathering ($^{187}Os/^{188}Os$ = 1.540), hydrothermal input ($^{187}Os/^{188}Os$ = 0.129), and cosmic
122 input ($^{187}Os/^{188}Os$ = 0.126) (Pegram et al., 1992; Ravizza, 1993), of which continental weathering
123 contributes ~80%, and hydrothermal and cosmic sources account for ~20% (Sharma et al., 1997).
124 However, the seawater Os isotope composition may have been also influenced by additional factors,
125 including changes in hydrothermal activity (Sharma et al., 2000) and chemical weathering of
126 organic-rich sedimentary rocks such as black shales, which display high $^{187}Os/^{188}Os$ ratios and Os
127 contents nearly a thousand times higher than other rock types (Singh et al., 1999).
128 During chemical weathering and fluid transport, ^{6}Li preferentially enters into the solid products
129 of weathering such as secondary clay minerals, while ^{7}Li preferentially remains in the fluid phase,
130 which results in a large Li isotope fractionation during weathering (Dellinger et al., 2015; Huh et
131 al., 1998; Lemarchand et al., 2010). There are two main sources of Li to seawater: fluvial input and
132 hydrothermal input (Huh et al., 1998; Weldeghebriel and Lowenstein, 2023). Marine sediment
133 records of seawater Li isotopes during the Cenozoic document an increase in $\delta^{7}Li$ values, which has
134 been interpreted as reflecting enhanced silicate weathering due to tectonic uplift (Misra and Froelich,
135 2012). Other factors that likely influenced the seawater $\delta^{7}Li$ evolution include: (1) the boomerang-

shape response of riverine δ^7Li values to weathering intensity, with a rise and then a fall with increasing weathering intensity (Dellinger et al., 2015), such that the riverine δ^7Li values in high-denudation uplifted regions is lower; and (2) shifts in weathering regimes, such as the expansion of floodplains downstream of mountain belts, which can generate higher riverine δ^7Li values (Pogge von Strandmann and Henderson, 2015).

Concerning Be, meteoric cosmogenic ^{10}Be is formed at a relatively constant production rate by the interactions of high-energy cosmic-ray particles with oxygen and nitrogen atoms in the atmosphere (Raisbeck and Yiou, 1984). In contrast, ^{9}Be in seawater mainly derives from dissolved riverine inputs, thereby serving as a tracer for continental chemical weathering (Willenbring and von Blanckenburg, 2010). The seawater ^{10}Be/^{9}Be ratio, after correction for ^{10}Be decay with a half-life of 1.387 Ma (Chmeleff et al., 2010; Korschinek et al., 2010), has therefore been used to reconstruct continental weathering fluxes during the late Cenozoic (Willenbring and von Blanckenburg, 2010). The residence time of Be in the ocean is about 200–1000 yr (Lao et al., 1992; von Blanckenburg et al., 1996), which is short enough for it to respond sensitively to continental weathering fluxes over relatively short timescales. However, this proxy also has some challenges: (1) the scavenging and/or release of ^{9}Be in estuarine and near-shore settings may limit the sensitivity of seawater ^{10}Be/^{9}Be ratios to changes in continental weathering fluxes (Deng et al., 2023; Li et al., 2021); and (2) the short ocean residence time of Be leads to a spatially heterogeneous isotopic distribution, which could therefore be affected by changes in ocean currents (Raisbeck and Yiou, 1984).

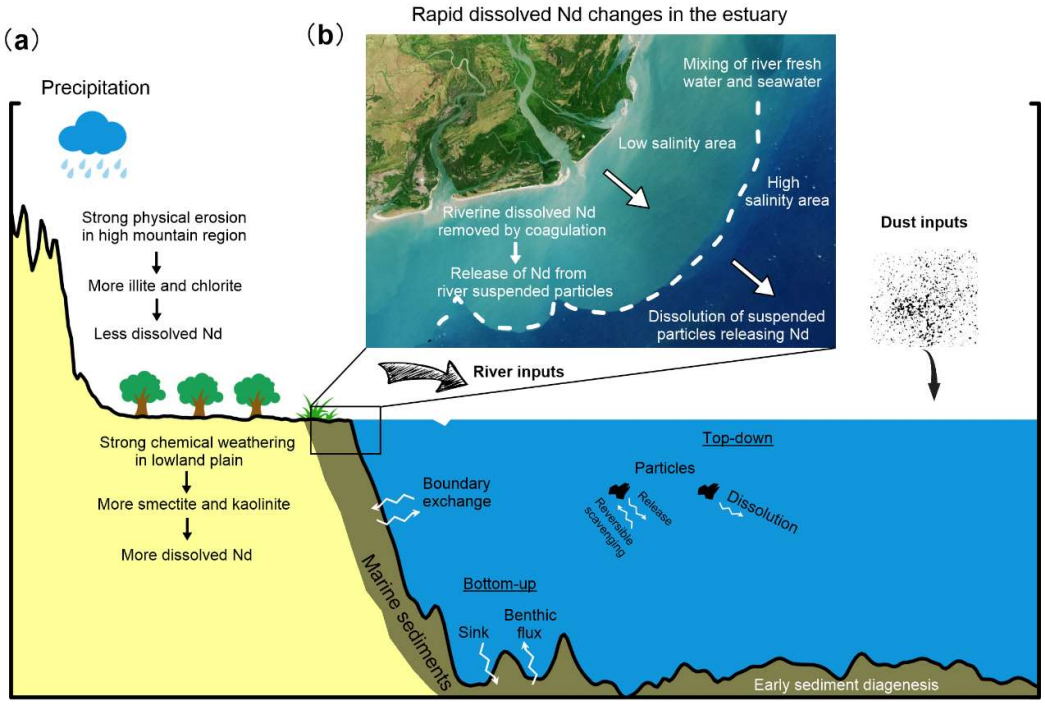

Figure 1. Schematic diagrams of (a) the sources and behaviour of Nd in seawater, and (b) the estuarine processes acting upon riverine Nd inputs.

3. Neodymium isotopes in seawater

3.1 Seawater Nd isotopes as a tracer of water masses and continental weathering

The Nd isotope composition ($\varepsilon_{Nd} = [(^{143}Nd/^{144}Nd)_{sample}/(^{143}Nd/^{144}Nd)_{CHUR} - 1] \times 10^4$) of seawater also has the potential to provide valuable insights into continental weathering (Jacobsen and Wasserburg, 1980). On a basin scale, the dissolved ε_{Nd} distribution is similar to conservative circulation tracers, such as salinity, which indicates that ε_{Nd} is a good tracer of ocean circulation (von Blanckenburg, 1999). Moreover, Nd isotopes are not sensitive to biological processes and the composition of their inputs is not significantly influenced by grain-size effects or weathering intensity in most settings (Frank, 2002; Goldstein and Hemming, 2003). In the modern ocean, the residence time of Nd is ~ 200-1000 yr, which is shorter than the deep-ocean mixing time (Tachikawa et al., 1999). As such, the distribution of seawater Nd isotopes is spatially heterogeneous, ranging from ε_{Nd} −7 to 0 in the Pacific Ocean, between −10 and −5 in the Indian Ocean , and from −20 to

172 −10 in the Atlantic Ocean (Lacan et al., 2012; van de Flierdt et al., 2016; van de Flierdt et al., 2012).
173 On this basis, Nd isotopes in seawater and marine authigenic phases have been commonly used to
174 trace modern water mass mixing and paleo-circulation in the open ocean (Frank, 2002; Goldstein
175 and Hemming, 2003). For example, in the Atlantic Ocean, Nd isotopes have been used to reconstruct
176 the advection of deep water masses and corresponding overturning rates during the last deglacial
177 period (Arsouze et al., 2008; Blaser et al., 2019; Gu et al., 2017; Piotrowski et al., 2012; Pöppelmeier
178 et al., 2022; Roberts et al., 2010), past glacial-interglacial cycles (Dausmann et al., 2017; Farmer et
179 al., 2019; Howe et al., 2016; Pena and Goldstein, 2014; Pöppelmeier et al., 2021), and over million-
180 year timescales (Batenburg et al., 2018; Khelifi and Frank, 2014; Kirby et al., 2020; Kirillova et al.,
181 2019). Over million-year timescales, Nd isotopes also reveal the timing of tectonic-driven opening
182 or closing of ocean passages via their impact on ocean circulation (Kirillova et al., 2019; Scher and
183 Martin, 2006). Additionally, major shifts in seawater Nd isotope composition have been used to
184 infer periods of enhanced weathering inputs following the emplacement of volcanic arcs,
185 demonstrating past linkages between chemical weathering of mafic rocks and global cooling over
186 geologic timescales (Bayon et al., 2023b; Conwell et al., 2022).
187 In early works, the Nd isotope composition of seawater was reconstructed from Fe-Mn crusts
188 (Abouchami et al., 1999; Albarède and Goldstein, 1992; Frank, 2002; Ling et al., 1997; von
189 Blanckenburg, 1999), which grow slowly at rates of a few mm per million years, and hence typically
190 provide records of past seawater Nd isotopes over million-year timescales. To investigate the
191 evolution of seawater ε_{Nd} values over centennial to orbital timescales, researchers have applied Nd
192 isotopes to fossil fish teeth (apatite) (Huck et al., 2016; Martin and Haley, 2000), foraminifera (Hu
193 and Piotrowski, 2018; Hu et al., 2016b; Palmer and Elderfield, 1985; Roberts et al., 2012; Tachikawa

et al., 2014; Vance et al., 2004; Wu et al., 2015), and deep-sea corals (Copard et al., 2010; Van de Flierdt et al., 2010). Acid-reductive sediment leaching was also developed to extract the dispersed authigenic Fe-Mn oxyhydroxide phases from marine sediment cores, which greatly improved the resolution and flexibility of Nd isotope reconstructions, addressing issues such as the absence of foraminifera in cores from below the carbonate compensation depth (Bayon et al., 2002; Du et al., 2020; Gutjahr et al., 2007; Rutberg et al., 2000). In detail, and depending on the sedimentological setting, the leaching solution chemistry, concentration, and leaching time are important factors in obtaining reliable reconstructions using this approach, while comparison with other robust carriers such as foraminifera and fish teeth can also serve as support to ensure the reliability of leachate data (Blaser et al., 2016; Du et al., 2016; Wilson et al., 2013).

Foraminifera are widely regarded as a reliable carrier for the Nd isotope composition of past seawater (Palmer and Elderfield, 1985; Tachikawa et al., 2014; Wilson et al., 2013; Wu et al., 2015). Initially, it was considered that oxidative-reductive cleaning could effectively remove Fe-Mn oxides and other components from the shells of planktonic foraminifera, such that the Nd in cleaned planktonic foraminifera would mainly derive from the carbonate shells and represent past surface water signals (Burton and Vance, 2000; Stoll et al., 2007; Vance and Burton, 1999). However, subsequent research found that the Fe-Mn oxide coatings could not be sufficiently removed and dominate the Nd budget even in cleaned foraminifera samples, such that planktonic foraminifera provide a bottom water or pore water signature, rather than a surface water signal (Kraft et al., 2013; Piotrowski et al., 2012; Roberts et al., 2012; Yu et al., 2018).

3.2 Sources of Nd isotopes in marginal seawater

Important progress has been made to understand the sources of dissolved Nd to seawater

(Figure 1). In the modern ocean, dissolved seawater Nd concentrations and isotopes are controlled by dissolved weathering inputs, dissolution of riverine and dust particles, adsorption/release by settling particles in seawater (Siddall et al., 2008), and benthic inputs from marine sediment (Abbott et al., 2015a; Abbott et al., 2015b; Deng et al., 2022; Haley et al., 2017; Lacan and Jeandel, 2005), as well as by water mass mixing.

In the open ocean, the distribution of dissolved Nd isotope compositions mainly arises from the mixing of different water masses tagged with distinctive ε_{Nd} signatures (von Blanckenburg, 1999), which provides a basis for tracing water mass mixing in the past. In contrast, marginal seas receive inputs of continentally-derived dissolved Nd from rivers and from submarine groundwater discharge, as well as experiencing strong particulate-seawater interactions, which lead to non-conservative behaviour of Nd isotopes in seawater (Elderfield et al., 1990; Johannesson and Burdige, 2007; Xu et al., 2023). Previous studies have demonstrated that the dissolved and particulate riverine inputs to the ocean display different behaviour (Jeandel et al., 2007; Sholkovitz and Szymczak, 2000). Typically, more than 70% of the dissolved riverine input of Nd is removed by the coagulation processes of riverine colloidal matter in river mouths (Elderfield et al., 1990; Sholkovitz, 1993). Meanwhile, the riverine particles, and especially suspended clays, can remain in the water column, or at the seawater-sediment interface, for a relatively long time, enabling Nd to be supplied to seawater by dissolution and/or exchange processes (Arsouze et al., 2009; Tachikawa et al., 2003). Therefore, dissolved riverine inputs presumably have a stronger influence on seawater Nd isotopes in the surface waters close to estuaries, while lithogenic riverine particles to control dissolved Nd inputs to intermediate and deep waters of marginal seas (Arsouze et al., 2009; Tachikawa et al., 2003). For example, a study in the Amazon estuary documented that Nd is mainly supplied by

terrigenous particles in high-salinity seawater on timescales of weeks, implying that the release of terrigenous particles is an important source of Nd to the ocean (Rousseau et al., 2015).

Boundary exchange processes may be important in providing dissolved Nd inputs to marginal seawater. This concept arose from the observation of changes in seawater Nd isotope composition (but little change in Nd concentrations) along a range of ocean margins, including the Northwestern Atlantic, Eastern Indian Ocean, and Western Equatorial Pacific (Lacan and Jeandel, 2005). To explain these changes, it was proposed that the sediment deposited along continental margins and/or suspended particles in the water column can release Nd into the ocean, hence modifying the Nd isotope composition of advected water masses, while also removing Nd from seawater by particle scavenging (Jeandel et al., 1998; Lacan and Jeandel, 2005). Note that the inputs and outputs of Nd may not always be in balance, and may be set by multiple processes, so the term 'boundary exchange' can be taken as the overall result of all above-mentioned processes, rather than relating to any single chemical process (Jeandel, 2016). Overall, this non-conservative behaviour limits our ability to use seawater Nd isotopes to track water mass mixing, particularly in marginal seas, while its influence varies regionally depending on the intensity of boundary exchange relative to water mass advection.

In detail, how sediment dissolution and release affect the dissolved Nd concentration and its isotopes in seawater remains to be fully understood (Du et al., 2025). One important process involved in boundary exchange is reversible scavenging, which allows Nd that is released in the surface ocean by desorption from, or dissolution of, riverine or dust particles to be scavenged and transported downwards by particles as they settle into the deep ocean (top-down hypothesis) (Siddall et al., 2008). In addition, dissolved Nd from the interstitial waters of seafloor sediments can be released into bottom water as benthic fluxes, before being transported through the water column by

diffusion (bottom-up hypothesis) (Du et al., 2025; Haley et al., 2017). A significant release of Nd from sediment interstitial waters to bottom waters has been revealed in multiple settings, including the California continental margin (Abbott et al., 2015b), the Tasman Sea (Abbott, 2019), and the Niger Delta area (Bayon et al., 2011). Extrapolating globally, such diffusive fluxes of Nd from seafloor pore fluids could potentially account for much of the missing Nd in global budgets (Arsouze et al., 2009), and thereby contribute to the previously-inferred boundary exchange. However, the budget of this benthic flux varies widely, with recent observations suggesting that it is a less significant process at the West Antarctic margin (Wang et al., 2022). As such, it needs to be assessed in further settings, where relevant controlling factors could include the sediment mineralogy, deposition rate, distance from estuaries, redox conditions, and flow speed. Finally, recent studies have provided support for the importance of diagenesis and the formation of authigenic clays in marine sediment as a potential source of rare earth elements, including Nd, to bottom waters (Abbott et al., 2022; Abbott, 2019; Bayon et al., 2023a); a process that will also require further investigation in future studies.

The above discussion demonstrates that seawater Nd isotopes in marginal seas are sensitive to a combination of dissolved and particulate riverine inputs, and particularly to fine-grained suspended sediment inputs. In this case, there is potential to use Nd isotopes as a tracer for the regional continental weathering inputs. Such an idea previously emerged in the interpretations of Pleistocene planktic foraminiferal Nd isotope records from the Labrador Sea (Vance and Burton, 1999) and Bay of Bengal (BoB) (Burton and Vance, 2000), but the potential link with weathering becomes more complex once they are interpreted as bottom water records. In the next section, we explore the possibility of using bottom water Nd isotope records to trace regional weathering inputs

in marginal seas based on a series of recent studies from the BoB.

In addition to changes in weathering inputs, changes in the mineralogical composition of terrigenous riverine inputs may have played a secondary role in controlling past seawater ε_{Nd} compositions at ocean margins (Huang et al., 2024). Specifically, investigations of marine sediment cores from the BoB document significant co-variability in clay mineral assemblages and seawater Nd isotopes over glacial-interglacial timescales, with interglacial periods being characterized by relatively high (smectite+kaolinite)/(illite+chlorite) ratios and low (unradiogenic) ε_{Nd} values, and vice-versa (Huang et al., 2024). In South Asian river systems, illite and chlorite mainly derive from physical erosion of igneous or sedimentary rocks in the high-elevation catchment regions associated with limited chemical weathering (Huyghe et al., 2011; Sarin et al., 1989). Hence, the illite and chlorite-dominated assemblages from glacial periods were probably produced from less weathered sediments eroded by Himalayan glaciers (Yu et al., 2020; Zhao et al., 2019). In contrast, smectite and kaolinite are mainly formed as a result of intense chemical weathering in the Indo-Gangetic floodplain (Sarin et al., 1989) (Figure 1). The occurrence of higher (smectite+kaolinite)/(illite+chlorite) ratios in interglacial (e.g., MIS 1 and 5) sediment intervals in the BoB was therefore consistent with contemporaneous intensification of summer monsoon rainfall (Colin et al., 1999; Yu et al., 2020).

The above observations have led to the proposal that mature clay mineral assemblages, such as smectite and kaolinite (and other pedogenic minerals), are more prone to releasing and/or exchanging Nd with seawater than immature assemblages dominated by illite and chlorite e. In the South China Sea, kaolinite and smectite with high degree of chemical weathering were also argued to be more efficient in releasing Nd into the seawater than less weathered illite and chlorite (Huang

et al., 2023). This hypothesis is further supported by recent findings showing that the preferential dissolution of kaolinite and the subsequent Fe-bearing clay authigenesis at ocean margins can release rare earth elements to seawater (Bayon et al., 2023a), a process that would require further investigation in future studies to assess its possible link with the evolution of seawater ε_{Nd}.

4. Neodymium isotopes tracing continental weathering inputs: a case study from the Bay of Bengal

The BoB is an ideal marginal sea for verifying the extent to which Nd isotopes in seawater can be used to trace continental weathering inputs. First, it is a semi-enclosed marginal sea that receives significant seasonal weathering inputs of both dissolved and particulate matter from the Ganga-Brahmaputra (G-B) river system, which largely dominate over riverine inputs from other small rivers in the region. Second, the ε_{Nd} composition of the weathering inputs delivered by the G-B river (ε_{Nd} values from −18 to −14) (Colin et al., 1999; Singh and France-Lanord, 2002) is distinct from the seawater ε_{Nd} values advected to the BoB from the south (ε_{Nd} values from −9 to −7) (Amakawa et al., 2019; van de Flierdt et al., 2016), providing good sensitivity to resolve their mixing. Finally, dissolved Nd isotopes in the BoB have been shown to derive predominantly from water mass mixing and lithogenic particulate input, whereas the release of Nd from pore water is only a secondary source in this region (Nozaki and Alibo, 2003; Yu et al., 2017b).

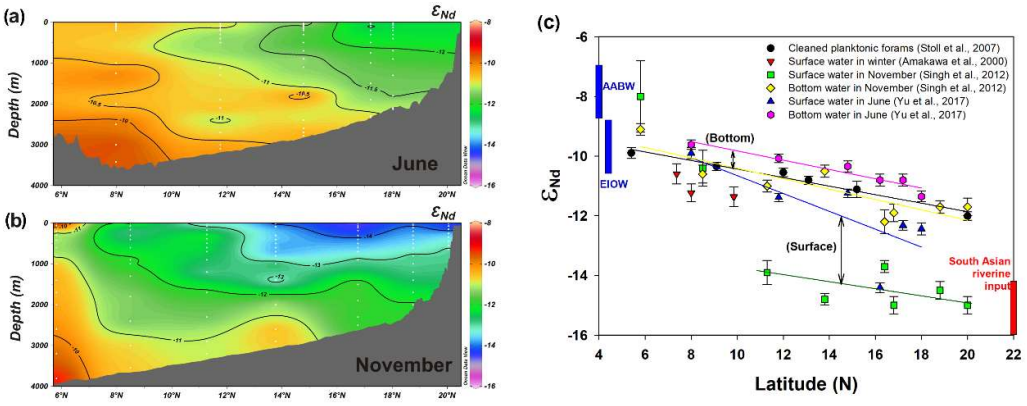

Figure 2. Modern spatial patterns and temporal changes in dissolved seawater Nd isotopes in the BoB (Yu et al., 2018; Yu et al., 2017b). (a) Water column of the 89°E transect from June 2012. (b) Water column of the 87°E transect from November 2008. (c) Coretop planktonic foraminiferal ε_{Nd} values (Stoll et al., 2007) compared to bottom and surface water ε_{Nd} values in a transect through the BoB. Modified based on (Amakawa et al., 2000; Singh et al., 2012; Yu et al., 2018; Yu et al., 2017b). Black arrows indicate the seasonal offsets for surface water and bottom water. AABW, Antarctic Bottom Water; EIOW, Eastern Indian Ocean Surface Water.

4.1 Modern seawater Nd isotopes in the Bay of Bengal

Dissolved Nd isotopes and concentrations were analysed in waters collected in winter from several stations in the BoB to study the influences of water mass mixing and weathering inputs (Singh et al., 2012). Those authors found a strong latitudinal gradient in Nd isotopes from unradiogenic waters in the north to more radiogenic waters in the south, in both surface and bottom waters, which was interpreted as reflecting a decreasing influence of riverine inputs from the G-B river system from north to south (Singh et al., 2012) (Figure 2b and c). A model calculation suggested that the contribution of particulate Nd from the G-B river and northern marginal sediments to the dissolved Nd budget in the BoB varies spatially, from 1% up to 65% (Singh et al., 2012). Sediment traps in the northern BoB showed that the particulate inputs from the G-B river to the BoB range from ~ 20 mg/m^2/d in winter to ~ 60 mg/m^2/d in summer due to the enhanced summer monsoon precipitation (Unger et al., 2003). Because the dissolution and exchange of Nd between sediment particles and seawater occurs over timescales of several weeks (Rousseau et al., 2015; Singh et al., 2012), such seasonal variations in the lithogenic particulate input are expected to have an important impact on dissolved Nd isotopes in the BoB (Yu et al., 2017b).

To explore potential seasonality, a second set of seawater samples along an ~89°E transect was collected from the BoB in June 2012, a period which corresponds to the onset of the summer monsoon rainfall (Yu et al., 2017b). A north–south gradient for Nd isotopes was observed in both

surface and bottom waters, and was particularly pronounced in the surface waters, which ranged from ε_{Nd} values of −14.4 in the northern BoB to −9.9 in the southern BoB (Figure 2a and c). Compared to the samples collected in November 2008 (Singh et al., 2012), the June 2012 samples had more radiogenic ε_{Nd} values by ~ 2 ε_{Nd} for the water shallower than 2000 m, and by ~ 0.5 ε_{Nd} for waters below 2000 m (black arrows in Figure 2c), together with lower Nd concentrations by ~5 pmol/kg (Singh et al., 2012; Yu et al., 2017b). Although the possibility that spatial differences in seawater Nd isotopic composition may exist between sampling locations, the large ε_{Nd} discrepancy in the surface water between June (early monsoon) and November (post-monsoon) (Figure 2c) is best explained as reflecting seasonal weathering inputs linked to monsoonal precipitation (Yu et al., 2017b). This observation suggests that the distribution of dissolved Nd isotopes in the BoB (and probably other marginal seas) fluctuates over seasonal timescales through changes in riverine input fluxes (Singh et al., 2012; Yu et al., 2017b), albeit considering that there is a four-month delay between the peak of G–B river discharge and the corresponding river plume area and associated unradiogenic ε_{Nd} signature in the BoB (Yu et al., 2017b). Moreover, the reduction of several pmol/kg in Nd concentrations near the seawater-sediment interface (Singh et al., 2012; Yu et al., 2017a) was potentially related to the removal of Nd associated with inorganic particle scavenging (Nozaki and Alibo, 2003; Singh et al., 2012; Yu et al., 2017b). This observation suggests that sediment interstitial water is not a major source of Nd to bottom seawater in the BoB. An insignificant role for benthic fluxes is also suggested by the lack of ^{228}Ra (an indicator for the diffusion of elements from sediment pore water into seawater) in the deep waters of the BoB (Moore and Santschi, 1986; Nozaki and Alibo, 2003). Hence, the above observations together indicate that the BoB represents an ideal location for exploring seawater Nd isotope changes in response to continental weathering inputs.

Overall, the distribution pattern of seawater ε_{Nd} in the BoB shows clear north-south variability (Figure 2c), which mainly reflects the mixing of unradiogenic inputs from regional rivers (ε_{Nd} values from −18 to −14), dominated by the G-B, with the radiogenic Eastern Indian Ocean Surface Water (ε_{Nd} values from −10 to −9) or Antarctic Bottom Water (AABW; ε_{Nd} values from −9 to −7) (Goswami et al., 2012; Piepgras and Wasserburg, 1982; Yu et al., 2017b). In addition, the unradiogenic ε_{Nd} signature extends further south into the open ocean at intermediate water depths (Figure 2a and b), possibly because the dissolution and scavenging of suspended particles reaches a threshold at these depths (Singh et al., 2012; Yu et al., 2017b). Hence, sediment cores from intermediate water depths in the BoB may be more sensitive than deeper cores for tracing weathering inputs with Nd isotopes.

Moreover, the coretop foraminiferal ε_{Nd} values in the BoB agree with the bottom water signal north of 10°N, and are inconsistent with the surface water ε_{Nd} values, regardless of the season (Stoll et al., 2007) (Figure 2c). South of 10°N, the foraminiferal ε_{Nd} values in the BoB are consistent with both surface and bottom water (Figure 2c), because the water column is more homogenous, presumably reflecting the significantly reduced influence of dissolved riverine Nd inputs. Overall, this comparison provides high confidence in the use of planktonic foraminifera in the BoB sediment cores as an archive of past bottom water Nd isotope compositions, and supports interpreting such records in terms of bottom water compositions rather than as local porewater compositions.

4.2 Past seawater Nd isotope composition in the Bay of Bengal over millennial and orbital timescales

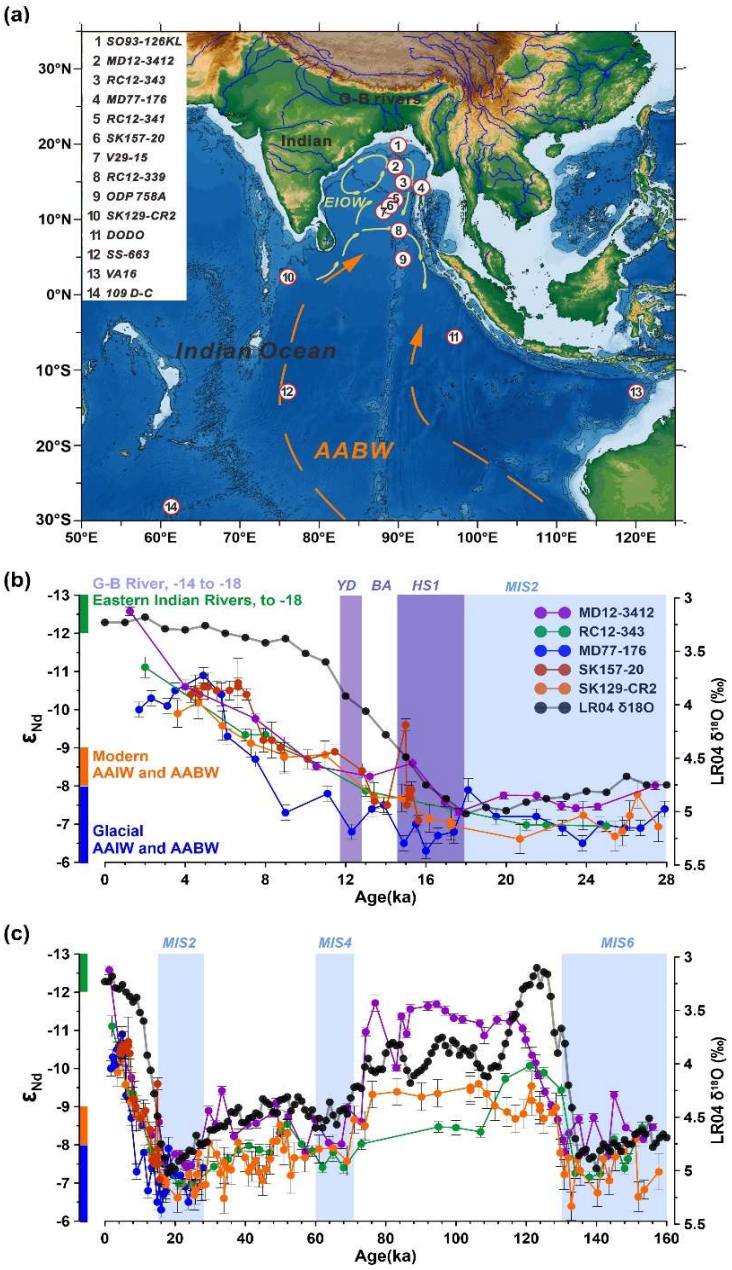

Figure 3. (a) Map of sediment cores (1-10) and ferromanganese crusts (11-14) from the BoB and the Indian Ocean discussed in this study. (b) Millennial and (c) glacial-interglacial timescale Nd isotope records from the BoB compared to the compositions of water masses and riverine inputs. The purple bars indicate millennial-scale cold events, and the light blue bars indicate cold marine isotope stages. All records are from mixed planktonic foraminifers, except for SK157-20 (mixed planktonic and benthic foraminifers) and SK129-CR2 (decarbonated sediment leachates). Further information and references for the cores are given in Table 1. References for Nd inputs: modern and glacial Antarctic Intermediate Water (AAIW) (Amakawa et al., 2019; Hu et al., 2016a; van de Flierdt et al., 2016); Antarctic Bottom Water (AABW) (Amakawa et al., 2019; Basak et al., 2015; Stichel et al., 2012; van de Flierdt et al., 2016); Ganga-Brahmaputra (G-B) River (Lupker et al., 2013; Singh and France-Lanord, 2002); Eastern Indian Rivers: Godavari and Krishna Rivers (Ahmad et al.,

2009), Deccan Traps (Dessert et al., 2001; Lightfoot and Hawkesworth, 1988), Peninsular Gneisses (Goswami et al., 2012). YD, Younger Dryas; BA, Bølling-Allerød; HS 1, Heinrich Stadial 1; MIS, marine isotope stage.

Table 1 Locations and references for the sediment cores and ferromanganese crusts discussed in this study.

No.	Sites	Latitude (°N)	Longitude (°E)	Depth (m)	References
1	SO93-126KL	20.0	90.0	-1253	(Stoll et al., 2007)
2	MD12-3412	17.2	89.5	-2383	(Huang et al., 2024)
3	RC12-343	15.2	90.6	-2666	(Stoll et al., 2007)
4	MD77-176	14.3	93.1	-1375	(Yu et al., 2018)
5	RC12-341	13.1	89.6	-2988	(Stoll et al., 2007)
6	SK157-20	12.1	88.7	-3171	(Naik et al., 2019)
7	V29-15	12.0	88.7	-3173	(Stoll et al., 2007)
8	RC12-339	9.1	90.0	-3010	(Stoll et al., 2007)
9	ODP 758A	5.4	90.4	-2925	(Gourlan et al., 2008; Gourlan et al., 2010; Song et al., 2023; Stoll et al., 2007)
10	SK129-CR2	3.0	76.0	-3800	(Piotrowski et al., 2009; Wilson et al., 2015)
11	DODO	-5.4	97.5	-4119	(Frank et al., 2006)
12	SS-663	-13.0	76.0	-5300	(O'Nions et al., 1998)
13	VA16	-12.9	119.9	-2100	(Frank et al., 2006)
14	109D-C	-28.0	61.0	-5200	(O'Nions et al., 1998)

To explore the past changes in seawater Nd isotopes in the BoB on millennial and orbital timescales, we compiled a selection of published continuous authigenic Nd isotope records in Figure 3. Similar long-term variations in both the amplitude and pattern of changes are observed in several cores from the BoB, both on millennial and orbital timescales (Figure 3), despite them being marked by distinct detrital Nd isotope signatures, sediment accumulation rates, and lithologic characteristics. This observation hints at the reliability of these records as archives of past seawater composition. In core MD77-176, slightly more radiogenic ε_{Nd} values are observed during the cold Heinrich Stadial 1 (HS 1) and Younger Dryas (YD) periods compared to the warm intervening Bølling-Allerød (BA) period, with an amplitude of ~1 ε_{Nd} unit (Figure 3b). However, in general, there is no

418 prominent millennial-scale variability in the authigenic Nd isotope records from the BoB (Figure
419 3b), which is probably due to the limited temporal resolution of the records and/or a buffered
420 temporal response of weathering inputs to the millennial-scale fluctuations in the summer monsoon.
421 In contrast, distinct glacial-interglacial variations are observed in the same records (Figure 3c).
422 Unradiogenic Nd isotope values are observed during interglacial periods, with ε_{Nd} values falling
423 between ~ −10 and −12 during Marine Isotope Stages (MIS) 1 and 5 (Figure 3b). Comparatively
424 more radiogenic Nd isotope values of ~ −7 to −8 are observed during all glacial periods (MIS 2, 4,
425 and 6). These results indicate a consistent Nd isotope regional shift of ~2 to 5 ε_{Nd} units during glacial-
426 interglacial transitions (Burton and Vance, 2000; Huang et al., 2024; Naik et al., 2019; Piotrowski
427 et al., 2009; Stoll et al., 2007; Wilson et al., 2015; Yu et al., 2018). Notably, the absolute ε_{Nd} values
428 are somewhat offset from the composition of deep southern-sourced water masses during this
429 interval, with ε_{Nd} values of −8.5 to −6.5 indicated by a foraminiferal Nd isotope record from the
430 southern Indian Ocean (Williams et al., 2021), and show larger temporal variations. Hence, such
431 glacial-interglacial ε_{Nd} variations in the BoB, and particularly the 4 to 5 ε_{Nd} unit variations at the
432 most northerly cores (Huang et al., 2024), cannot be explained only by changes in the water mass
433 compositions advected from the Southern Ocean. Since the timing of the glacial-interglacial
434 variations in the BoB corresponds closely with the global oxygen isotope curve (Lisiecki and Raymo,
435 2005; Stoll et al., 2007) (Figure 3c) and with changes in the South Asian summer monsoon intensity
436 (Yu et al., 2020), we infer that changes in unradiogenic Nd inputs linked to continental weathering,
437 in phase with summer monsoon precipitation, exerted a major control on those records.

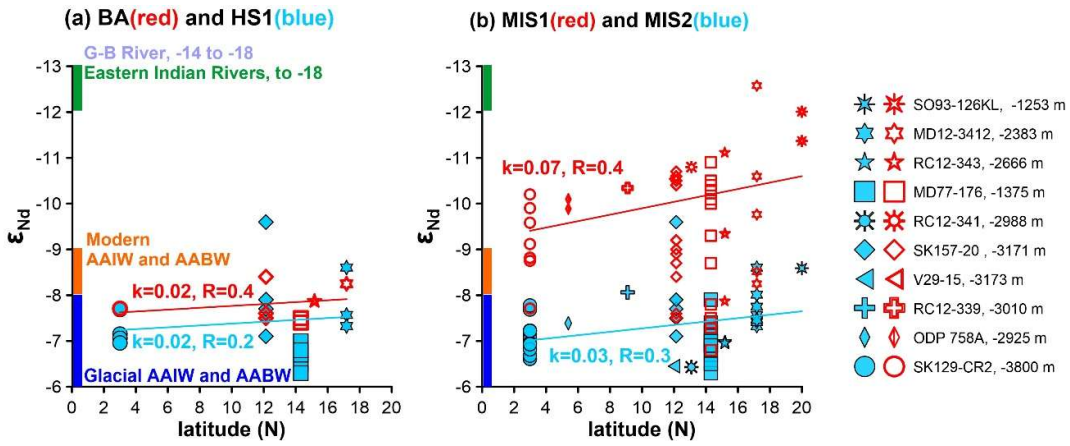

Figure 4. Past seawater Nd isotopes versus latitude in the BoB. (a) Comparison between the BA (14.6-12.8 ka BP) and HS 1 (18-14.6 ka BP). (b) Comparison between MIS 1 (14.6 ka BP - present) and MIS 2 (28-14.6 ka BP). The fit lines were calculated based on the mean ε_{Nd} values in each core; k is the slope of the linear fit (y = -kx + b), and R is the correlation coefficient. References for the cores and the sediment/water mass endmembers are found in Figure 3 and Table 1.

To assess the influence of riverine weathering inputs on the millennial-scale and orbital-scale Nd isotope variability, we plot Nd isotopes versus latitude for all published data in Figure 4. As also shown in Figure 3, the ε_{Nd} changes on glacial-interglacial timescales (~2.5 ε_{Nd} units) are significantly larger than those on millennial timescales (~0.5 ε_{Nd} units). In addition to the potential inability of these BoB sediment cores to record short-lived climate events, this observation would also be consistent with the Indian summer monsoon intensity and the corresponding weathering inputs varying more on orbital timescales than on millennial timescales. In addition, glacial-interglacial changes in the Nd isotope composition of Southern Ocean water mass advected northward could also influence the seawater ε_{Nd} proxy records (Wilson et al., 2015; Yu et al., 2022), particularly at the more southerly core locations. Considering the uncertainty in in discriminating between advected and weathering signals, the spatial Nd isotope gradient provides additional constraints. Notably, the latitudinal ε_{Nd} gradient is approximately constant on millennial timescales (Figure 4a), while the gradient during interglacial MIS 1 (k = 0.07 ε_{Nd}/degree) is significantly greater than that

during glacial MIS 2 (k = 0.03 ε_{Nd}/degree) (Figure 4b), which strongly points to enhanced unradiogenic Nd inputs from riverine sources during interglacial periods.

4.3 Variability of seawater Nd isotopes in the Bay of Bengal on tectonic timescales

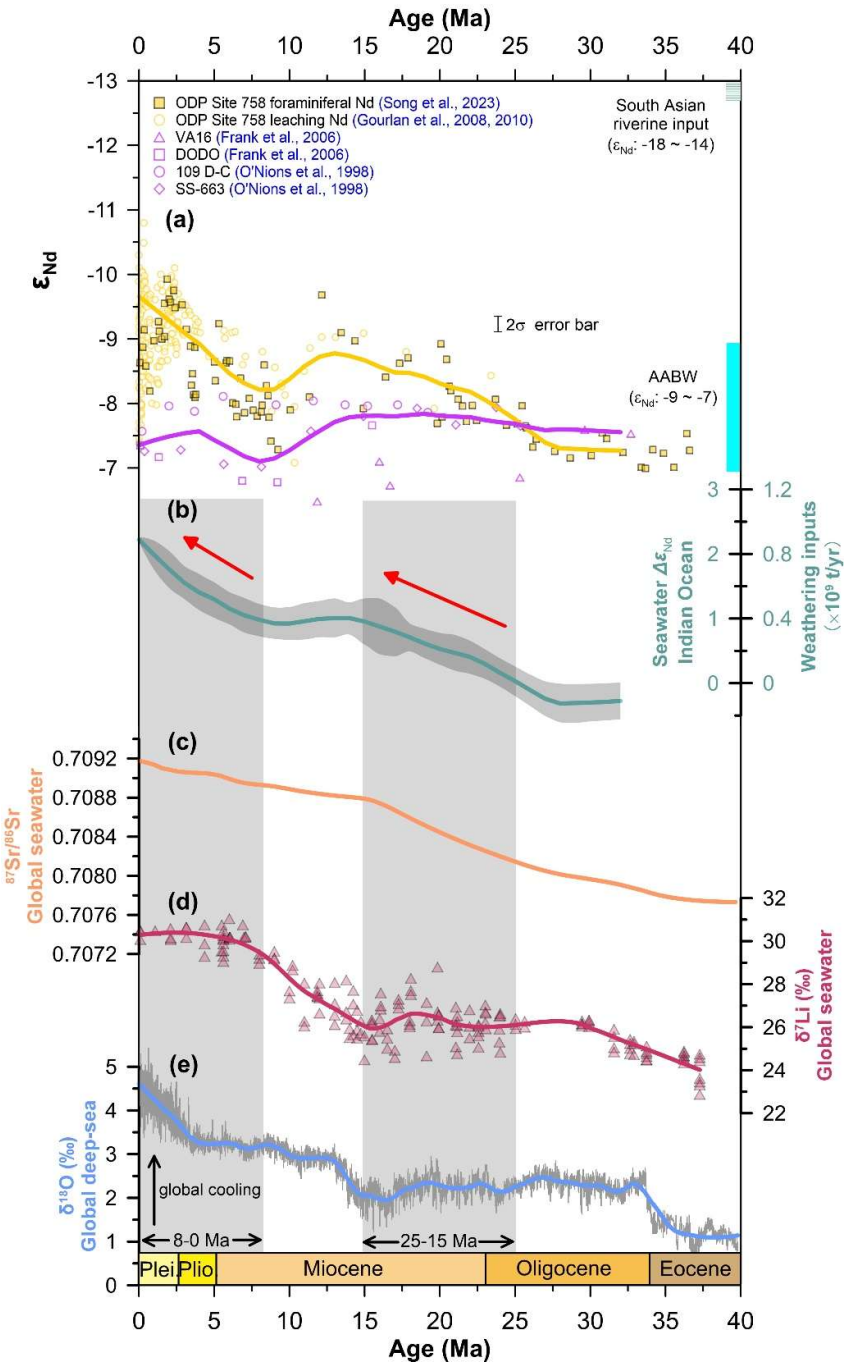

Figure 5. Comparison of seawater Nd isotope records from the BoB with other climatic records (Song et al., 2023). (a) Seawater Nd isotope records from the northern Indian Ocean (ODP Site 758)

and central Indian Ocean (ferromanganese crusts) since the late Eocene (Song et al., 2023). Ochre and purple lines represent the bottom seawater Nd isotope evolution in the northern and central Indian Ocean, respectively, using a LOESS smoothing method with parameters of 0.3. (b) Blue line represents an estimate for South Asian weathering inputs based on the latitudinal seawater Nd isotope gradient ($\Delta\varepsilon_{Nd}$) between the two curves in panel (a), with grey shading representing its error range (Song et al., 2023). (c) Continental weathering proxy based on the seawater $^{87}Sr/^{86}Sr$ record (McArthur et al., 2020). (d) Continental weathering proxy based on the foraminiferal $\delta^{7}Li$ record (Misra and Froelich, 2012). (e) Global climate change based on the deep-sea benthic $\delta^{18}O$ stack, reflecting a combination of deep-ocean temperature and ice volume (Westerhold et al., 2020). Abbreviations: Plei, Pleistocene; Plio, Pliocene. References for the cores and the sediment/water mass endmembers are found in Figure 3 and Table 1. Grey shaded bars indicate two intervals of inferred increases in weathering inputs.

Studies reconstructing seawater Nd isotopes in the BoB on million-year timescales have mostly been based on ODP Site 758 in the southern BoB. Such records, based on sediment leachates and planktonic foraminifera, show a long-term decrease in ε_{Nd} values from approximately −7 during the late Eocene to −10 in the present day (Gourlan et al., 2008; Gourlan et al., 2010; Song et al., 2023) (Figure 5a). Given the more limited changes in the Nd isotope composition of the deep Indian Ocean at more southerly upstream sites (Frank et al., 2006; O'Nions et al., 1998) (Figure 5a), these results suggest that the deep water in the BoB has been increasingly influenced by unradiogenic Nd from South Asian riverine inputs towards the present day. In turn, the increased terrigenous input of dissolved and/or particulate-associated Nd can be attributed to tectonic activity and climatic change in South Asia since the late Cenozoic (Clift et al., 2008; Derry and France-Lanord, 1997; Mutz et al., 2018).

To better assess the variations in continental weathering inputs from South Asia, the $\Delta\varepsilon_{Nd}$ proxy was proposed based on the Nd isotope gradient between the central Indian Ocean and ODP Site 758 from the southern BoB (Song et al., 2023). Reconstructions from ferromanganese crusts from deep water in the central Indian Ocean constrain the composition of Indian Ocean deep waters since 33

492 Ma (mainly AABW), which ranged from ε_{Nd} values of −8.5 to −6.5 (Frank et al., 2006; O'Nions et
493 al., 1998) (Figure 5a). These data suggest that the deep Indian Ocean was generally filled by AABW
494 since the Oligocene, with the modern AABW ε_{Nd} value ranging between −9 and −7 (Amakawa et
495 al., 2019; van de Flierdt et al., 2016). Although those reconstructions from ferromanganese crusts
496 give comparable ε_{Nd} values to the modern AABW, more studies are needed to constrain the temporal
497 evolution of the AABW endmember composition and its flow strength into the Indian Ocean since
498 the Oligocene. For example, a weakening in AABW flow strength could have increased the $\Delta\varepsilon_{Nd}$
499 gradient independent of changes in continental weathering inputs. Nevertheless, in the absence of
500 strong evidence for changing AABW flow strength, the increase in the $\Delta\varepsilon_{Nd}$ gradient towards the
501 present day suggests a sustained enhancement of weathering inputs from the South Asian continent
502 and the Himalayas since the Oligocene (Figure 5b).

503 Moreover, the inferred link between the Himalayan evolution and the $\Delta\varepsilon_{Nd}$ record is also
504 supported by the similarity between the variations in $\Delta\varepsilon_{Nd}$ and the long-term evolution of Sr isotopes
505 in seawater since the late Eocene (Figure 5c), for which a link to the Himalayas is well established
506 (McArthur et al., 2020; Song et al., 2023). In contrast, and unsurprisingly given the differences
507 between the Sr and Li isotope curves, there are discrepancies in the timing of the changes in the
508 $\Delta\varepsilon_{Nd}$ record and the global seawater Li isotope evolution (Misra and Froelich, 2012; Song et al.,
509 2023) (Figure 5d). Such discrepancies could reflect the complex controls on the composition of Li
510 isotope inputs to the ocean (Pogge von Strandmann and Henderson, 2015), or could simply arise
511 because the seawater Li isotope record is sensitive to global budgets while the $\Delta\varepsilon_{Nd}$ record reflects
512 regional changes in continental weathering inputs to the Indian Ocean. In addition, the $\Delta\varepsilon_{Nd}$ record
513 could also reflect changes in continental erosion fluxes or in the type of clay minerals being

delivered, whereas the Li isotope curve is likely more closely related to dissolved inputs. Overall, this example demonstrates that seawater Nd isotope records have the potential to trace changes in continental weathering inputs on million-year tectonic timescales, providing an opportunity to explore the links between tectonics, climate, and weathering changes, which may be further assessed using records from marginal seas in other global settings.

4.5 Quantification of past weathering inputs in the Bay of Bengal using seawater Nd isotopes

In this section, we attempt to obtain an empirical relationship based on modern weathering inputs and changes in seawater Nd isotopes in the BoB, and apply it to quantify past weathering changes based on the million-year evolution of Nd isotopes in Indian Ocean records.

We start by considering a mass balance approach, using the Himalayan weathering inputs (w) and southern-sourced waters (s) in a simple two-endmember mixing calculation (Yu et al., 2022). For a starting point at 0 Ma,

$$(\varepsilon_{Nd})_{Wo}[Nd]_{Wo}F_{wo} + (\varepsilon_{Nd})_{So}[Nd]_{So}(1 - F_{wo}) = (\varepsilon_{Nd})_{Ao}([Nd]_{Wo} + [Nd]_{So}) \quad \text{(Eq. 1)}$$

For any time of x Ma,

$$(\varepsilon_{Nd})_{Wx}[Nd]_{Wx}F_{wx} + (\varepsilon_{Nd})_{Sx}[Nd]_{Sx}(1 - F_{wx}) = (\varepsilon_{Nd})_{Ax}([Nd]_{Wx} + [Nd]_{Sx}) \quad \text{(Eq. 2)}$$

Here, F_w indicates the contributed proportion of weathering inputs; $(\varepsilon_{Nd})_W$, $(\varepsilon_{Nd})_S$, and $(\varepsilon_{Nd})_A$ correspond to the Nd isotope compositions of regional weathering inputs, southern-sourced waters, and authigenic (foraminiferal) values, respectively; and $[Nd]_W$ and $[Nd]_S$ represent the Nd fluxes for the regional weathering inputs and southern-sourced waters contributing to bottom water at the location of the authigenic Nd record. To simplify, we consider that the $(\varepsilon_{Nd})_S$ *and* $[Nd]_S$ for the southern-sourced waters remained largely constant over tectonic timescales, (i.e. $(\varepsilon_{Nd})_{So}$

$\approx (\varepsilon_{Nd})_{Sx}$ and $[Nd]_{So} \approx [Nd]_{Sx}$), compared to the regional weathering inputs (Amakawa et al., 2019; van de Flierdt et al., 2016) (Figure 3 and 5), hence meaning that long-term seawater Nd isotope variability in the BoB is mostly driven by changes in regional weathering inputs. Subtracting equation 1 from equation 2, and assuming that the $(\varepsilon_{Nd})_W$ of the regional weathering inputs is also stable through time (i. e. $(\varepsilon_{Nd})_{Wo} \approx (\varepsilon_{Nd})_{Wx}$) (France-Lanord et al., 1993), we obtain the following equation:

$$(\varepsilon_{Nd})_W([Nd]_{Wx} - [Nd]_{Wo}) = ((\varepsilon_{Nd})_{Ax} - (\varepsilon_{Nd})_{Ao})([Nd]_{Wx} + [Nd]_S) \quad \text{(Eq. 3)}$$

Considering that $([Nd]_{Wx} - [Nd]_{Wo})$ is generally smaller in magnitude than $([Nd]_{Wx} + [Nd]_S)$, to a first approximation we can consider $([Nd]_{Wx} + [Nd]_S)$ as invariable. With this simplification, changes in the regional weathering input flux $([Nd]_{Wx} - [Nd]_{Wo})$ are linearly related to the difference in seawater ε_{Nd} values from measurements at the two times $((\varepsilon_{Nd})_{Ax} - (\varepsilon_{Nd})_{Ao})$.

Here, we obtain an empirical version of that relationship based on the modern Himalayan weathering input flux and the shift in Nd isotope composition between the modern AABW and the core-top authigenic value at ODP Site 758. The difference between AABW ($\varepsilon_{Nd} = -7$) (Hu et al., 2016a; Stichel et al., 2012) and the core-top value at ODP Site 758 ($\varepsilon_{Nd} = -10$) (Song et al., 2023) is ~ 3 ε_{Nd} units (Figure 5), which corresponds to an average riverine sediment input of 1.1 x10^9 t/year, when considering only the input from the G-B river (which is an order of magnitude greater than that of all the rivers of the eastern Indian Peninsula) (Milliman and Syvitski, 1992; Unger et al., 2003). Based on the empirical approach described above, we can convert any $\Delta\varepsilon_{Nd}$ change at the BoB ODP Site 758 since 32 Ma into varying weathering inputs (Figure 5b). This reconstruction indicates that Himalayan weathering inputs gradually increased from the late Oligocene (~25 Ma),

reaching approximately half their modern level by the middle Miocene (~15 Ma) (Figure 5). After a ~7 Ma period of stability, those inputs began to increase rapidly again since the late Miocene (~8 Ma) until they reached the level of modern weathering inputs in the late Pleistocene (Figure 5). We acknowledge that the above assessment of past Himalayan weathering inputs only represents a first-order semi-quantitative estimate based on many assumptions, and that conducting a true statistical error analysis of these findings would be irrelevant. Further studies will be required to assess past variations in the composition and respective contribution of the different weathering endmembers, and to better understand the processes transferring continental weathering geochemical signals into the deep ocean, and to thereby further refine the relationship between Nd isotope changes and weathering inputs.

5. Conclusions and implications

This review has focused on the potential of using past seawater Nd isotope reconstructions from marginal seas as a tool to assess past continental weathering inputs. Taking the BoB as an example, we have explored what we can learn about changes in continental weathering inputs over seasonal, millennial, orbital, and million-year timescales, and have drawn the following conclusions. Weathering inputs from large Himalayan river systems controlled by seasonal monsoon precipitation, such as the Ganga-Brahmaputra River, can drive regional changes in seawater Nd isotopes at the spatial scale of marginal basins such as the BoB. Over glacial-interglacial timescales, seawater Nd isotopes in the BoB display significant variability, associated with pronounced changes in monsoon-driven riverine inputs and/or changes in the mineralogical composition of the sediment load, as well as changes in the composition of deep waters advected from the Southern Ocean. In contrast, changes of seawater Nd isotopes in the BoB are less evident on millennial timescales,

likely related to processes buffering weathering inputs and/or their archiving in the marine record. A long-term shift towards more unradiogenic seawater Nd isotope compositions in the BoB since the Oligocene reveals a strong influence of South Asian continental weathering inputs related to Himalayan tectonic uplift and monsoonal precipitation, providing an opportunity to explore the links between tectonics, climate, and weathering.

In contrast to other weathering proxies such as Sr, Os, Li, but like Be isotopes, seawater Nd isotope records can only trace regional weathering inputs due to its short ocean residence time (<1 kyr). The advantage brought by this feature is that seawater Nd isotopes can be used to distinguish the strength of weathering inputs from different continental or island regions. Apart from the BoB, this approach has been applied successfully to other marginal seas such as the south China Sea (Li et al., 2025) and the northeastern Indian Ocean (Bayon et al., 2023b). Nevertheless, future investigations should aim at acquiring additional seawater Nd isotope records from different marginal seas to address the long-term evolution of oceanic Nd isotopes, and inferred chemical weathering signals, at a global scale. Further research is also required to better understand the processes controlling the distribution of Nd isotopes in seawater, such as the influence of sediment mineralogy, early diagenesis, sedimentation rate, and seafloor redox conditions on the boundary exchange and benthic fluxes.

Acknowledgements

This study was supported by the National Natural Science Foundation of China (42376055, 42125602, W2421051 and 42076052), the Strategic Priority Research Program of the Chinese Academy of Sciences (XDB40010100 and XDB42010402), the Natural Science Foundation of Shandong (ZR2022YQ33), National Key Research and Development Program of China

(2022YFF0800503), and the Taishan Scholars Program (tsqn202507275). DJW was supported by a Natural Environment Research Council independent research fellowship (NE/T011440/1). We thank the editor and three anonymous reviewers for their constructive comments that improved the manuscript. For the purpose of open access, the authors have applied a Creative Commons Attribution (CC BY) licence to any Author Accepted Manuscript version arising.

Data availability: Seawater Nd isotopes data in the Northern Indian Ocean is available in Zenodo: https://doi.org/10.5281/zenodo.17773016.

References

Abbott, A., Löhr, S., Payne, A., Kumar, H., Du, J., 2022. Widespread lithogenic control of marine authigenic neodymium isotope records? Implications for paleoceanographic reconstructions. Geochimica et Cosmochimica Acta 319, 318–336.

Abbott, A.N., 2019. A benthic flux from calcareous sediments results in non-conservative neodymium behavior during lateral transport: A study from the Tasman Sea. Geology 47(4), 363–366.

Abbott, A.N., Haley, B.A., McManus, J., 2015a. Bottoms up: Sedimentary control of the deep North Pacific Ocean's εNd signature. Geology 43(11), 1035–1035.

Abbott, A.N., Haley, B.A., McManus, J., Reimers, C.E., 2015b. The sedimentary flux of dissolved rare earth elements to the ocean. Geochimica et Cosmochimica Acta 154, 186–200.

Abouchami, W., Galer, S., Koschinsky, A., 1999. Pb and Nd isotopes in NE Atlantic Fe–Mn crusts: proxies for trace metal paleosources and paleocean circulation. Geochimica et Cosmochimica Acta 63(10), 1489–1505.

Ahmad, S.M., Padmakumari, V., Babu, G.A., 2009. Strontium and neodymium isotopic compositions in sediments from Godavari, Krishna and Pennar rivers. Current science 97(12).

Albarède, F., Goldstein, S.L., 1992. World map of Nd isotopes in sea-floor ferromanganese deposits. Geology 20(8), 761–763.

Amakawa, H., Alibo, D.S., Nozaki, Y., 2000. Nd isotopic composition and REE pattern in the surface waters of the eastern Indian Ocean and its adjacent seas. Geochimica et Cosmochimica Acta 64(10), 1715–1727.

Amakawa, H., Yu, T.-L., Tazoe, H., Obata, H., Gamo, T., Sano, Y., Shen, C.-C., Suzuki, K., 2019. Neodymium concentration and isotopic composition distributions in the southwestern Indian Ocean and the Indian sector of the Southern Ocean. Chemical Geology 511, 190–203. doi.org/https://doi.org/10.1016/j.chemgeo.2019.01.007.

Arnscheidt, C.W., Rothman, D.H., 2022. Presence or absence of stabilizing Earth system feedbacks on different time scales. Science Advances 8(46), eadc9241.

Arsouze, T., Dutay, J., Lacan, F., Jeandel, C., 2009. Reconstructing the Nd oceanic cycle using a coupled dynamical-biogeochemical model. Biogeosciences 6(12), 2829–2846.

Arsouze, T., Dutay, J.C., Kageyama, M., Lacan, F., 2008. Influence of the Atlantic thermohaline

circulation on neodymium isotopic composition at the Last Glacial Maximum – a modelling sensitivity study. Climate of the Past Discussions 4(2), 309–333.
Basak, C., Pahnke, K., Frank, M., Lamy, F., Gersonde, R., 2015. Neodymium isotopic characterization of Ross Sea Bottom Water and its advection through the southern South Pacific. Earth and Planetary Science Letters 419, 211–221.
Bastian, L., Revel, M., Bayon, G., Dufour, A., Vigier, N., 2017. Abrupt response of chemical weathering to Late Quaternary hydroclimate changes in northeast Africa. Scientific Reports 7, 44231. doi.org/10.1038/srep44231
https://www.nature.com/articles/srep44231#supplementary-information.
Batenburg, S.J., Voigt, S., Friedrich, O., Osborne, A.H., Bornemann, A., Klein, T., Pérez-Díaz, L., Frank, M., 2018. Major intensification of Atlantic overturning circulation at the onset of Paleogene greenhouse warmth. Nature Communications 9(1), 4954.
Bayon, G., Birot, D., Ruffine, L., Caprais, J.-C., Ponzevera, E., Bollinger, C., Donval, J.-P., Charlou, J.-L., Voisset, M., Grimaud, S., 2011. Evidence for intense REE scavenging at cold seeps from the Niger Delta margin. Earth and Planetary Science Letters 312(3), 443–452.
Bayon, G., German, C., Boella, R., Milton, J., Taylor, R., Nesbitt, R., 2002. An improved method for extracting marine sediment fractions and its application to Sr and Nd isotopic analysis. Chemical Geology 187(3-4), 179–199.
Bayon, G., Giresse, P., Chen, H., Rouget, M.-L., Gueguen, B., Moizinho, G.R., Barrat, J.-A., Beaufort, D., 2023a. The Behavior of Rare Earth Elements during Green Clay Authigenesis on the Congo Continental Shelf. Minerals 13(8), 1081.
Bayon, G., Lambert, T., Vigier, N., De Deckker, P., Freslon, N., Jang, K., Larkin, C.S., Piotrowski, A.M., Tachikawa, K., Thollon, M., 2020. Rare earth element and neodymium isotope tracing of sedimentary rock weathering. Chemical Geology 553, 119794.
Bayon, G., Patriat, M., Godderis, Y., Trinquier, A., De Deckker, P., Kulhanek, D.K., Holbourn, A., Rosenthal, Y., 2023b. Accelerated mafic weathering in Southeast Asia linked to late Neogene cooling. Science Advances 9(13), eadf3141.
Beaulieu, E., Goddéris, Y., Donnadieu, Y., Labat, D., Roelandt, C., 2012. High sensitivity of the continental-weathering carbon dioxide sink to future climate change. Nature Climate Change 2, 346. doi.org/10.1038/nclimate1419
https://www.nature.com/articles/nclimate1419#supplementary-information.
Berner, R.A., Lasaga, A.C., Garrels, R.M., 1983. Carbonate-silicate geochemical cycle and its effect on atmospheric carbon dioxide over the past 100 million years. Am. J. Sci.;(United States) 283(7).
Blaser, P., Lippold, J., Gutjahr, M., Frank, N., Link, J.M., Frank, M., 2016. Extracting foraminiferal seawater Nd isotope signatures from bulk deep sea sediment by chemical leaching. Chemical Geology 439, 189–204.
Blaser, P., Pöppelmeier, F., Schulz, H., Gutjahr, M., Frank, M., Lippold, J., Heinrich, H., Link, J., Hoffmann, J., Szidat, S., 2019. The resilience and sensitivity of Northeast Atlantic deep water εNd to overprinting by detrital fluxes over the past 30,000 years. Geochimica et cosmochimica acta 245, 79–97.
Blum, J.D., 1997. The effect of late Cenozoic glaciation and tectonic uplift on silicate weathering rates and the marine 87 Sr/86 Sr record. Tectonic uplift and climate change, 259–288.
Bouchez, J., Gaillardet, J., Lupker, M., Louvat, P., France-Lanord, C., Maurice, L., Armijos, E., Moquet, J.-S., 2012. Floodplains of large rivers: weathering reactors or simple silos? Chemical Geology 332, 166–184.

Bufe, A., Rugenstein, J.K., Hovius, N., 2024. CO2 drawdown from weathering is maximized at moderate erosion rates. Science 383(6687), 1075–1080.

Burton, K.W., Vance, D., 2000. Glacial–interglacial variations in the neodymium isotope composition of seawater in the Bay of Bengal recorded by planktonic foraminifera. Earth and Planetary Science Letters 176(3), 425–441.

Chmeleff, J., von Blanckenburg, F., Kossert, K., Jakob, D., 2010. Determination of the ^{10}Be half-life by multicollector ICP-MS and liquid scintillation counting. Nuclear Instruments and Methods in Physics Research Section B: Beam Interactions with Materials and Atoms 268(2), 192–199. doi.org/https://doi.org/10.1016/j.nimb.2009.09.012.

Clift, P., Jonell, T., Du, Y., Bornholdt, T., 2024. The impact of Himalayan-Tibetan erosion on silicate weathering and organic carbon burial. Chemical Geology 656, 122106. doi.org/https://doi.org/10.1016/j.chemgeo.2024.122106.

Clift, P.D., Hodges, K.V., Heslop, D., Hannigan, R., Van Long, H., Calves, G., 2008. Correlation of Himalayan exhumation rates and Asian monsoon intensity. Nature Geoscience 1(12), 875–880.

Colbourn, G., Ridgwell, A., Lenton, T., 2015. The time scale of the silicate weathering negative feedback on atmospheric CO2. Global Biogeochemical Cycles 29(5), 583–596.

Colin, C., Turpin, L., Bertaux, J., Desprairies, A., Kissel, C., 1999. Erosional history of the Himalayan and Burman ranges during the last two glacial–interglacial cycles. Earth and Planetary Science Letters 171(4), 647–660.

Conwell, C.T., Saltzman, M.R., Edwards, C.T., Griffith, E.M., Adiatma, Y.D., 2022. Nd isotopic evidence for enhanced mafic weathering leading to Ordovician cooling. Geology 50(8), 886–890.

Coogan, L.A., Dosso, S.E., 2015. Alteration of ocean crust provides a strong temperature dependent feedback on the geological carbon cycle and is a primary driver of the Sr-isotopic composition of seawater. Earth and Planetary Science Letters 415, 38–46. doi.org/10.1016/j.epsl.2015.01.027.

Copard, K., Colin, C., Douville, E., Freiwald, A., Gudmundsson, G., De Mol, B., Frank, N., 2010. Nd isotopes in deep-sea corals in the North-eastern Atlantic. Quaternary Science Reviews 29(19), 2499–2508.

Dalton, C.A., Wilson, D.S., Herbert, T.D., 2022. Evidence for a Global Slowdown in Seafloor Spreading Since 15 Ma. Geophysical Research Letters 49(6), e2022GL097937. doi.org/https://doi.org/10.1029/2022GL097937.

Dausmann, V., Frank, M., Gutjahr, M., Rickli, J., 2017. Glacial reduction of AMOC strength and long-term transition in weathering inputs into the Southern Ocean since the mid-Miocene: Evidence from radiogenic Nd and Hf isotopes. Paleoceanography 32(3), 265–283.

Dellinger, M., Gaillardet, J., Bouchez, J., Calmels, D., Louvat, P., Dosseto, A., Gorge, C., Alanoca, L., Maurice, L., 2015. Riverine Li isotope fractionation in the Amazon River basin controlled by the weathering regimes. Geochimica et Cosmochimica Acta 164, 71–93.

Deng, K., Rickli, J., Suhrhoff, T.J., Du, J., Scholz, F., Severmann, S., Yang, S., McManus, J., Vance, D., 2023. Dominance of benthic fluxes in the oceanic beryllium budget and implications for paleo-denudation records. Science Advances 9(23), eadg3702. doi.org/doi:10.1126/sciadv.adg3702.

Deng, K., Yang, S., Du, J., Lian, E., Vance, D., 2022. Dominance of benthic flux of REEs on continental shelves: implications for oceanic budgets. Geochemical Perspectives Letters 22, 26–30.

Derry, L.A., France-Lanord, C., 1997. Himalayan weathering and erosion fluxes: climate and tectonic controls, Tectonic uplift and climate change. Springer, pp. 289–312.

Dessert, C., Dupré, B., François, L.M., Schott, J., Gaillardet, J., Chakrapani, G., Bajpai, S., 2001. Erosion

of Deccan Traps determined by river geochemistry: impact on the global climate and the 87 Sr/86 Sr ratio of seawater. Earth and Planetary Science Letters 188(3), 459–474.
Dosseto, A., Vigier, N., Joannes-Boyau, R., Moffat, I., Singh, T., Srivastava, P., 2015. Rapid response of silicate weathering rates to climate change in the Himalaya. Geochemical Perspectives Letters 1(0), 10–19. doi.org/http://dx.doi.org/10.7185/geochemlet.1502.
Du, J., Haley, B.A., McManus, J., Blaser, P., Rickli, J., Vance, D., 2025. Abyssal seafloor as a key driver of ocean trace-metal biogeochemical cycles. Nature, 1–8.
Du, J., Haley, B.A., Mix, A.C., 2016. Neodymium isotopes in authigenic phases, bottom waters and detrital sediments in the Gulf of Alaska and their implications for paleo-circulation reconstruction. Geochimica et Cosmochimica Acta 193, 14–35.
Du, J., Haley, B.A., Mix, A.C., 2020. Evolution of the Global Overturning Circulation since the Last Glacial Maximum based on marine authigenic neodymium isotopes. Quaternary Science Reviews 241, 106396. doi.org/https://doi.org/10.1016/j.quascirev.2020.106396.
Edmond, J., 1992. Himalayan tectonics, weathering processes, and the strontium isotope record in marine limestones. Science 258(5088), 1594–1597.
Elderfield, H., Upstill-Goddard, R., Sholkovitz, E., 1990. The rare earth elements in rivers, estuaries, and coastal seas and their significance to the composition of ocean waters. Geochimica et Cosmochimica Acta 54(4), 971–991.
Farmer, J., Hönisch, B., Haynes, L., Kroon, D., Jung, S., Ford, H., Raymo, M., Jaume-Seguí, M., Bell, D., Goldstein, S., 2019. Deep Atlantic Ocean carbon storage and the rise of 100,000-year glacial cycles. Nature Geoscience 12(5), 355–360.
France-Lanord, C., Derry, L., Michard, A., 1993. Evolution of the Himalaya since Miocene time: isotopic and sedimentological evidence from the Bengal Fan. Geological Society, London, Special Publications 74(1), 603–621.
Frank, M., 2002. Radiogenic isotopes: tracers of past ocean circulation and erosional input. Reviews of Geophysics 40(1), 1–1–1–38. doi.org/https://doi.org/10.1029/2000RG000094.
Frank, M., Whiteley, N., van de Flierdt, T., Reynolds, B.C., O'Nions, K., 2006. Nd and Pb isotope evolution of deep water masses in the eastern Indian Ocean during the past 33 Myr. Chemical Geology 226(3-4), 264–279.
Gislason, S.R., Oelkers, E.H., Eiriksdottir, E.S., Kardjilov, M.I., Gisladottir, G., Sigfusson, B., Snorrason, A., Elefsen, S., Hardardottir, J., Torssander, P., 2009. Direct evidence of the feedback between climate and weathering. Earth and Planetary Science Letters 277(1-2), 213–222.
Goldstein, S.L., Hemming, S.R., 2003. Long-lived isotopic tracers in oceanography, paleoceanography, and ice-sheet dynamics. Treatise on geochemistry 6, 625.
Goswami, V., Singh, S.K., Bhushan, R., Rai, V.K., 2012. Temporal variations in $^{87}Sr/^{86}Sr$ and εNd in sediments of the southeastern Arabian Sea: Impact of monsoon and surface water circulation. Geochemistry, Geophysics, Geosystems 13(1).
Gourlan, A.T., Meynadier, L., Allègre, C.J., 2008. Tectonically driven changes in the Indian Ocean circulation over the last 25 Ma: Neodymium isotope evidence. Earth & Planetary Science Letters 267(1-2), 353–364.
Gourlan, A.T., Meynadier, L., Allègre, C.J., Tapponnier, P., Birck, J.-L., Joron, J.-L., 2010. Northern Hemisphere climate control of the Bengali rivers discharge during the past 4 Ma. Quaternary science reviews 29(19), 2484–2498.
Gu, S., Liu, Z., Zhang, J., Rempfer, J., Joos, F., Oppo, D.W., 2017. Coherent response of Antarctic

Intermediate Water and Atlantic Meridional Overturning Circulation during the last deglaciation: reconciling contrasting neodymium isotope reconstructions from the tropical Atlantic. Paleoceanography 32(10), 1036–1053.

Gutjahr, M., Frank, M., Stirling, C.H., Klemm, V., Van de Flierdt, T., Halliday, A.N., 2007. Reliable extraction of a deepwater trace metal isotope signal from Fe–Mn oxyhydroxide coatings of marine sediments. Chemical Geology 242(3-4), 351–370.

Haley, B.A., Du, J., Abbott, A.N., McManus, J., 2017. The impact of benthic processes on rare earth element and neodymium isotope distributions in the oceans. Frontiers in Marine Science 4, 426.

Hodell, D.A., Mead, G.A., Mueller, P.A., 1990. Variation in the strontium isotopic composition of seawater (8 Ma to present): Implications for chemical weathering rates and dissolved fluxes to the oceans. Chemical Geology: Isotope Geoscience section 80(4), 291–307.

Horan, K., Hilton, R.G., Selby, D., Ottley, C.J., Gröcke, D.R., Hicks, M., Burton, K.W., 2017. Mountain glaciation drives rapid oxidation of rock-bound organic carbon. Science Advances 3(10), e1701107. doi.org/10.1126/sciadv.1701107.

Howe, J.N., Piotrowski, A.M., Noble, T.L., Mulitza, S., Chiessi, C.M., Bayon, G., 2016. North Atlantic Deep Water Production during the Last Glacial Maximum. Nature Communications 7, 11765.

Hu, R., Noble, T.L., Piotrowski, A.M., Mccave, I.N., Bostock, H.C., Neil, H.L., 2016a. Neodymium isotopic evidence for linked changes in Southeast Atlantic and Southwest Pacific circulation over the last 200 kyr. Earth and Planetary Science Letters 455, 106–114.

Hu, R., Piotrowski, A.M., 2018. Neodymium isotope evidence for glacial-interglacial variability of deepwater transit time in the Pacific Ocean. Nature Communications 9(1), 4709.

Hu, R., Piotrowski, A.M., Bostock, H.C., Crowhurst, S., Rennie, V., 2016b. Variability of neodymium isotopes associated with planktonic foraminifera in the Pacific Ocean during the Holocene and Last Glacial Maximum. Earth and Planetary Science Letters 447, 130–138.

Huang, Y., Colin, C., Bassinot, F., Yu, Z., Dubois-Dauphin, Q., Dapoigny, A., Wilson, D.J., Bayon, G., 2024. Impact of riverine sediment mineralogy on seawater Nd isotope compositions in the northeastern part of the Indian Ocean during the last two glacial cycles. Earth and Planetary Science Letters 643, 118902.

Huang, Y., Colin, C., Liu, Z., Douville, E., Dapoigny, A., Haurine, F., Wu, Q., Tien-Shun Lin, A., 2023. Impacts of nepheloid layers and mineralogical compositions of oceanic margin sediments on REE concentrations and Nd isotopic compositions of seawater. Geochimica et Cosmochimica Acta 359, 57–70. doi.org/https://doi.org/10.1016/j.gca.2023.08.026.

Huck, C.E., van de Flierdt, T., Jiménez-Espejo, F.J., Bohaty, S.M., Röhl, U., Hammond, S.J., 2016. Robustness of fossil fish teeth for seawater neodymium isotope reconstructions under variable redox conditions in an ancient shallow marine setting. Geochemistry, Geophysics, Geosystems 17(3), 679–698.

Huh, Y., Chan, L.-H., Zhang, L., Edmond, J.M., 1998. Lithium and its isotopes in major world rivers: implications for weathering and the oceanic budget. Geochimica et Cosmochimica Acta 62(12), 2039–2051.

Huyghe, P., Guilbaud, R., Bernet, M., Galy, A., Gajurel, A.P., 2011. Significance of the clay mineral distribution in fluvial sediments of the Neogene to Recent Himalayan Foreland Basin (west-central Nepal). Basin Research 23(3), 332–345.

Jacobsen, S.B., Wasserburg, G., 1980. Sm-Nd isotopic evolution of chondrites. Earth and Planetary Science Letters 50(1), 139–155.

Jeandel, Arsouze, T., Lacan, F., Techine, P., Dutay, J.-C., 2007. Isotopic Nd compositions and

concentrations of the lithogenic inputs into the ocean: A compilation, with an emphasis on the margins. Chemical Geology 239(1), 156–164.
Jeandel, C., 2016. Overview of the mechanisms that could explain the 'Boundary Exchange'at the land–ocean contact. Philosophical Transactions of the Royal Society A: Mathematical, Physical and Engineering Sciences 374(2081), 20150287.
Jeandel, C., Thouron, D., Fieux, M., 1998. Concentrations and isotopic compositions of neodymium in the eastern Indian Ocean and Indonesian straits. Geochimica et Cosmochimica Acta 62(15), 2597–2607.
Johannesson, K.H., Burdige, D.J., 2007. Balancing the global oceanic neodymium budget: evaluating the role of groundwater. Earth and Planetary Science Letters 253(1-2), 129–142.
Khelifi, N., Frank, M., 2014. A major change in North Atlantic deep water circulation 1.6 million years ago. Climate of the Past 10(4), 1441–1451.
Kirby, N., Bailey, I., Lang, D.C., Brombacher, A., Chalk, T.B., Parker, R.L., Crocker, A.J., Taylor, V.E., Milton, J.A., Foster, G.L., 2020. On climate and abyssal circulation in the Atlantic Ocean during late Pliocene marine isotope stage M2,∼ 3.3 million years ago. Quaternary Science Reviews 250, 106644.
Kirillova, V., Osborne, A.H., Störling, T., Frank, M., 2019. Miocene restriction of the Pacific-North Atlantic throughflow strengthened Atlantic overturning circulation. Nature Communications 10(1), 4025.
Korschinek, G., Bergmaier, A., Faestermann, T., Gerstmann, U.C., Knie, K., Rugel, G., Wallner, A., Dillmann, I., Dollinger, G., von Gostomski, C.L., Kossert, K., Maiti, M., Poutivtsev, M., Remmert, A., 2010. A new value for the half-life of ^{10}Be by Heavy-Ion Elastic Recoil Detection and liquid scintillation counting. Nuclear Instruments and Methods in Physics Research Section B: Beam Interactions with Materials and Atoms 268(2), 187–191. doi.org/https://doi.org/10.1016/j.nimb.2009.09.020.
Kraft, S., Frank, M., Hathorne, E.C., Weldeab, S., 2013. Assessment of seawater Nd isotope signatures extracted from foraminiferal shells and authigenic phases of Gulf of Guinea sediments. Geochimica et Cosmochimica Acta 121, 414–435. doi.org/https://doi.org/10.1016/j.gca.2013.07.029.
Lacan, F., Jeandel, C., 2005. Neodymium isotopes as a new tool for quantifying exchange fluxes at the continent–ocean interface. Earth and Planetary Science Letters 232(3), 245–257.
Lacan, F., Tachikawa, K., Jeandel, C., 2012. Neodymium isotopic composition of the oceans: A compilation of seawater data. Chemical Geology 300, 177–184.
Lao, Y., Anderson, R.F., Broecker, W.S., Trumbore, S.E., Hofmann, H.J., Wolfli, W., 1992. Transport and burial rates of ^{10}Be and ^{231}Pa in the Pacific Ocean during the Holocene period. Earth and Planetary Science Letters 113(1), 173–189. doi.org/https://doi.org/10.1016/0012-821X(92)90218-K.
Lein, A.Y., 2004. Authigenic carbonate formation in the ocean. Lithology and Mineral Resources 39, 1–30.
Lemarchand, E., Chabaux, F., Vigier, N., Millot, R., Pierret, M.-C., 2010. Lithium isotope systematics in a forested granitic catchment (Strengbach, Vosges Mountains, France). Geochimica et Cosmochimica Acta 74(16), 4612–4628.
Li, M., Colin, C., Wan, S., Yu, Z., Jian, Z., Song, Z., Dapoigny, A., Jin, H., Zhang, J., Zhao, D., Li, A., 2025. Tectonics Modulated Long-Term Weathering Inputs From the East Asian Continent and Tropical Island Arc to the South China Sea Since the Late Oligocene. Geophysical Research Letters 52(10), e2024GL114500. doi.org/https://doi.org/10.1029/2024GL114500.
Li, S., Goldstein, S.L., Raymo, M.E., 2021. Neogene continental denudation and the beryllium conundrum. Proceedings of the National Academy of Sciences 118(42), e2026456118.
Lightfoot, P., Hawkesworth, C., 1988. Origin of Deccan Trap lavas: evidence from combined trace element and Sr-, Nd- and Pb-isotope studies. Earth & Planetary Science Letters 91(1), 89–104.

Ling, H., Burton, K., O'nions, R., Kamber, B., von Blanckenburg, F., Gibb, A., Hein, J., 1997. Evolution of Nd and Pb isotopes in Central Pacific seawater from ferromanganese crusts. Earth and Planetary Science Letters 146(1-2), 1–12.

Lisiecki, L., Raymo, M., 2005. A Pliocene-Pleistocene stack of 57 globally distributed benthic $\delta^{18}O$ records. Paleoceanography 20, PA1003.

Liu, W., Xu, Z., Jiang, H., Zhou, X., Zhao, T., Li, Y., 2023. Lithological and glacial controls on sulfide weathering and the associated CO2 budgets in the Tibetan Plateau: new constraints from small catchments. Geochimica et Cosmochimica Acta 343, 341–352.

Liu, W., Xu, Z., Sun, H., Zhao, M., Xu, Y., Guo, Z., 2025. Refined weathering CO2 budget of the Tibetan Plateau strongly modulated by sulphide oxidation. Nature Communications 16(1), 2741.

Lupker, M., France-Lanord, C., Galy, V., Lavé, J., Kudrass, H., 2013. Increasing chemical weathering in the Himalayan system since the Last Glacial Maximum. Earth and Planetary Science Letters 365, 243–252.

Martin, E., Haley, B., 2000. Fossil fish teeth as proxies for seawater Sr and Nd isotopes. Geochimica et Cosmochimica Acta 64(5), 835–847.

McArthur, J., Howarth, R., Shields, G., Zhou, Y., 2020. Strontium isotope stratigraphy, Geologic time scale 2020. Elsevier, pp. 211–238.

Milliman, J.D., Syvitski, J.P., 1992. Geomorphic/tectonic control of sediment discharge to the ocean: the importance of small mountainous rivers. The Journal of Geology, 525–544.

Miriyala, P., Sukumaran, N.P., Nath, B.N., Ramamurty, P.B., Sijinkumar, A.V., Vijayagopal, B., Ramaswamy, V., Sebastian, T., 2017. Increased chemical weathering during the deglacial to mid-Holocene summer monsoon intensification. Sci Rep 7, 44310.

Misra, S., Froelich, P.N., 2012. Lithium isotope history of Cenozoic seawater: changes in silicate weathering and reverse weathering. science 335(6070), 818–823.

Moore, W.S., Santschi, P.H., 1986. Ra-228 in the deep Indian Ocean. Deep Sea Research Part A. Oceanographic Research Papers 33(1), 107–120.

Mutz, S.G., Ehlers, T.A., Werner, M., Lohmann, G., Stepanek, C., Li, J., 2018. Estimates of late Cenozoic climate change relevant to Earth surface processes in tectonically active orogens. Earth Surf. Dynam. 6(2), 271–301. doi.org/10.5194/esurf-6-271-2018.

Naik, S.S., Basak, C., Goldstein, S.L., Naidu, P.D., Naik, S.N., 2019. A 16-kyr Record of Ocean Circulation and Monsoon Intensification From the Central Bay of Bengal. Geochemistry, Geophysics, Geosystems 20(2), 872–882. doi.org/https://doi.org/10.1029/2018GC007860.

Nozaki, Y., Alibo, D.S., 2003. Importance of vertical geochemical processes in controlling the oceanic profiles of dissolved rare earth elements in the northeastern Indian Ocean. Earth and Planetary Science Letters 205(3), 155–172.

O'Nions, R., Frank, M., von Blanckenburg, F., Ling, H.-F., 1998. Secular variation of Nd and Pb isotopes in ferromanganese crusts from the Atlantic, Indian and Pacific Oceans. Earth and Planetary Science Letters 155(1-2), 15–28.

Palmer, M., Elderfield, H., 1985. Variations in the Nd isotopic composition of foraminifera from Atlantic Ocean sediments. Earth and Planetary Science Letters 73(2-4), 299–305.

Pegram, W., Krishnaswami, S., Ravizza, G., Turekian, K., 1992. The record of sea water 187Os/186Os variation through the Cenozoic. Earth and Planetary Science Letters 113(4), 569–576.

Pena, L.D., Goldstein, S.L., 2014. Thermohaline circulation crisis and impacts during the mid-Pleistocene transition. Science 345(6194), 318–322.

Perri, F., 2020. Chemical weathering of crystalline rocks in contrasting climatic conditions using geochemical proxies: an overview. Palaeogeography, Palaeoclimatology, Palaeoecology 556, 109873.
Peucker-Ehrenbrink, B., Miller, M.W., Arsouze, T., Jeandel, C., 2010. Continental bedrock and riverine fluxes of strontium and neodymium isotopes to the oceans. Geochemistry, Geophysics, Geosystems 11(3).
Piepgras, D.J., Wasserburg, G.J., 1982. Isotopic Composition of Neodymium in Waters from the Drake Passage. Science 217(4556), 207–214.
Piotrowski, A., Galy, A., Nicholl, J., Roberts, N., Wilson, D., Clegg, J., Yu, J., 2012. Reconstructing deglacial North and South Atlantic deep water sourcing using foraminiferal Nd isotopes. Earth and Planetary Science Letters 357, 289–297.
Piotrowski, A.M., Banakar, V.K., Scrivner, A.E., Elderfield, H., Galy, A., Dennis, A., 2009. Indian Ocean circulation and productivity during the last glacial cycle. Earth and Planetary Science Letters 285(1), 179–189.
Pogge von Strandmann, P.A.E., Henderson, G.M., 2015. The Li isotope response to mountain uplift. Geology 43(1), 67–70. doi.org/10.1130/g36162.1.
Pöppelmeier, F., Gutjahr, M., Blaser, P., Schulz, H., Süfke, F., Lippold, J., 2021. Stable Atlantic deep water mass sourcing on glacial-interglacial timescales. Geophysical Research Letters 48(15), e2021GL092722.
Pöppelmeier, F., Lippold, J., Blaser, P., Gutjahr, M., Frank, M., Stocker, T.F., 2022. Neodymium isotopes as a paleo-water mass tracer: A model-data reassessment. Quaternary Science Reviews 279, 107404.
Quade, J., Roe, L., DeCelles, P.G., Ojha, T.P., 1997. The late Neogene 87Sr/86Sr record of lowland Himalayan rivers. Science 276(5320), 1828–1831.
Raisbeck, G.M., Yiou, F., 1984. Production of long-lived cosmogenic nuclei and their applications. Nuclear Instruments and Methods in Physics Research Section B: Beam Interactions with Materials and Atoms 5(2), 91–99. doi.org/https://doi.org/10.1016/0168-583X(84)90490-7.
Ravizza, G., 1993. Variations of the187Os/186Os ratio of seawater over the past 28 million years as inferred from metalliferous carbonates. Earth and Planetary Science Letters 118(1-4), 335–348.
Raymo, M., Ruddiman, W.F., 1992. Tectonic forcing of late Cenozoic climate. Nature 359(6391), 117–122.
Roberts, N.L., Piotrowski, A.M., Elderfield, H., Eglinton, T.I., Lomas, M.W., 2012. Rare earth element association with foraminifera. Geochimica et Cosmochimica Acta 94, 57–71.
Roberts, N.L., Piotrowski, A.M., McManus, J.F., Keigwin, L.D., 2010. Synchronous Deglacial Overturning and Water Mass Source Changes. Science 327(5961), 75–78. doi.org/10.1126/science.1178068.
Rousseau, T.C., Sonke, J.E., Chmeleff, J., van Beek, P., Souhaut, M., Boaventura, G., Seyler, P., Jeandel, C., 2015. Rapid neodymium release to marine waters from lithogenic sediments in the Amazon estuary. Nature communications 6.
Rutberg, R.L., Hemming, S.R., Goldstein, S.L., 2000. Reduced North Atlantic Deep Water flux to the glacial Southern Ocean inferred from neodymium isotope ratios. Nature 405(6789), 935–938.
Sarin, M., Krishnaswami, S., Dilli, K., Somayajulu, B., Moore, W., 1989. Major ion chemistry of the Ganga-Brahmaputra river system: Weathering processes and fluxes to the Bay of Bengal. Geochimica et cosmochimica acta 53(5), 997–1009.
Scher, H.D., Martin, E.E., 2006. Timing and Climatic Consequences of the Opening of Drake Passage. Science 312(5772), 428–430. doi.org/doi:10.1126/science.1120044.
Sharma, M., Papanastassiou, D., Wasserburg, G., 1997. The concentration and isotopic composition of

osmium in the oceans. Geochimica et Cosmochimica Acta 61(16), 3287–3299.
Sharma, M., Wasserburg, G., Hofmann, A., Butterfield, D., 2000. Osmium isotopes in hydrothermal fluids from the Juan de Fuca Ridge. Earth and Planetary Science Letters 179(1), 139–152.
Sholkovitz, E., Szymczak, R., 2000. The estuarine chemistry of rare earth elements: comparison of the Amazon, Fly, Sepik and the Gulf of Papua systems. Earth and Planetary Science Letters 179(2), 299–309.
Sholkovitz, E.R., 1993. The geochemistry of rare earth elements in the Amazon River estuary. Geochimica et Cosmochimica Acta 57(10), 2181–2190.
Siddall, M., Khatiwala, S., van de Flierdt, T., Jones, K., Goldstein, S.L., Hemming, S., Anderson, R.F., 2008. Towards explaining the Nd paradox using reversible scavenging in an ocean general circulation model. Earth and Planetary Science Letters 274(3), 448–461.
Singh, S.K., France-Lanord, C., 2002. Tracing the distribution of erosion in the Brahmaputra watershed from isotopic compositions of stream sediments. Earth and Planetary Science Letters 202(3), 645–662.
Singh, S.K., Trivedi, J., Krishnaswami, S., 1999. Re-Os isotope systematics in black shales from the Lesser Himalaya: Their chronology and role in the 187Os/188Os evolution of seawater. Geochimica et Cosmochimica Acta 63(16), 2381–2392.
Singh, S.P., Singh, S.K., Goswami, V., Bhushan, R., Rai, V.K., 2012. Spatial distribution of dissolved neodymium and εNd in the Bay of Bengal: role of particulate matter and mixing of water masses. Geochimica et Cosmochimica Acta 94, 38–56.
Song, Z., Wan, S., Colin, C., France-Lanord, C., Yu, Z., Dapoigny, A., Jin, H., Li, M., Zhang, J., Zhao, D., 2023. Enhanced weathering input from South Asia to the Indian Ocean since the late Eocene. Science Bulletin 68(3), 305–313.
Stichel, T., Frank, M., Rickli, J., Haley, B.A., 2012. The hafnium and neodymium isotope composition of seawater in the Atlantic sector of the Southern Ocean. Earth and Planetary Science Letters 317, 282–294.
Stoll, H.M., Vance, D., Arevalos, A., 2007. Records of the Nd isotope composition of seawater from the Bay of Bengal: Implications for the impact of Northern Hemisphere cooling on ITCZ movement. Earth and Planetary Science Letters 255(1), 213–228.
Tachikawa, K., Athias, V., Jeandel, C., 2003. Neodymium budget in the modern ocean and paleo-oceanographic implications. Journal of Geophysical Research: Oceans 108(C8).
Tachikawa, K., Jeandel, C., Roy-Barman, M., 1999. A new approach to the Nd residence time in the ocean: the role of atmospheric inputs. Earth and Planetary Science Letters 170(4), 433–446.
Tachikawa, K., Piotrowski, A.M., Bayon, G., 2014. Neodymium associated with foraminiferal carbonate as a recorder of seawater isotopic signatures. Quaternary Science Reviews 88, 1–13.
Torres, M.A., West, A.J., Clark, K.E., Paris, G., Bouchez, J., Ponton, C., Feakins, S.J., Galy, V., Adkins, J.F., 2016. The acid and alkalinity budgets of weathering in the Andes–Amazon system: Insights into the erosional control of global biogeochemical cycles. Earth and Planetary Science Letters 450, 381–391. doi.org/https://doi.org/10.1016/j.epsl.2016.06.012.
Torres, M.A., West, A.J., Li, G., 2014. Sulphide oxidation and carbonate dissolution as a source of CO_2 over geological timescales. Nature 507, 346. doi.org/10.1038/nature13030.
Unger, D., Ittekkot, V., Schäfer, P., Tiemann, J., Reschke, S., 2003. Seasonality and interannual variability of particle fluxes to the deep Bay of Bengal: influence of riverine input and oceanographic processes. Deep Sea Research Part II: Topical Studies in Oceanography 50(5), 897–923.
van de Flierdt, T., Griffiths, A.M., Lambelet, M., Little, S.H., Stichel, T., Wilson, D.J., 2016. Neodymium

in the oceans: a global database, a regional comparison and implications for palaeoceanographic research. Phil. Trans. R. Soc. A 374(2081), 20150293.
van de Flierdt, T., Pahnke, K., Amakawa, H., Andersson, P., Basak, C., Coles, B., Colin, C., Crocket, K., Frank, M., Frank, N., 2012. GEOTRACES intercalibration of neodymium isotopes and rare earth element concentrations in seawater and suspended particles. Part 1: reproducibility of results for the international intercomparison. Limnology and Oceanography: Methods 10(4), 234–251.
Van de Flierdt, T., Robinson, L.F., Adkins, J.F., 2010. Deep-sea coral aragonite as a recorder for the neodymium isotopic composition of seawater. Geochimica et Cosmochimica Acta 74(21), 6014–6032.
Vance, D., Burton, K., 1999. Neodymium isotopes in planktonic foraminifera: a record of the response of continental weathering and ocean circulation rates to climate change. Earth and Planetary Science Letters 173(4), 365–379.
Vance, D., Scrivner, A.E., Beney, P., Staubwasser, M., Henderson, G.M., Slowey, N.C., 2004. The use of foraminifera as a record of the past neodymium isotope composition of seawater. Paleoceanography 19(2).
Vance, D., Teagle, D.A.H., Foster, G.L., 2009. Variable Quaternary chemical weathering fluxes and imbalances in marine geochemical budgets. Nature 458, 493. doi.org/10.1038/nature07828 https://www.nature.com/articles/nature07828#supplementary-information.
von Blanckenburg, F., 1999. Tracing past ocean circulation? Science 286(5446), 1862.
von Blanckenburg, F., Bouchez, J., Ibarra, D.E., Maher, K., 2015. Stable runoff and weathering fluxes into the oceans over Quaternary climate cycles. Nature Geoscience 8, 538. doi.org/10.1038/ngeo2452 https://www.nature.com/articles/ngeo2452#supplementary-information.
von Blanckenburg, F., O'Nions, R.K., Belshaw, N.S., Gibb, A., Hein, J.R., 1996. Global distribution of beryllium isotopes in deep ocean water as derived from Fe-Mn crusts. Earth and Planetary Science Letters 141(1-4), 213–226.
Walker, J.C., Hays, P., Kasting, J.F., 1981. A negative feedback mechanism for the long-term stabilization of Earth's surface temperature. Journal of Geophysical Research: Oceans 86(C10), 9776–9782.
Wang, R., Williams, T.J., Hillenbrand, C.-D., Ehrmann, W., Larkin, C.S., Hutchings, A.M., Piotrowski, A.M., 2022. Boundary processes and neodymium cycling along the Pacific margin of West Antarctica. Geochimica et Cosmochimica Acta 327, 1–20.
Weldeghebriel, M.F., Lowenstein, T.K., 2023. Seafloor hydrothermal systems control long-term changes in seawater [Li⁺]: Evidence from fluid inclusions. Science Advances 9(30), eadf1605. doi.org/doi:10.1126/sciadv.adf1605.
West, A.J., 2012. Thickness of the chemical weathering zone and implications for erosional and climatic drivers of weathering and for carbon-cycle feedbacks. Geology 40(9), 811–814.
West, A.J., Galy, A., Bickle, M., 2005. Tectonic and climatic controls on silicate weathering. Earth and Planetary Science Letters 235(1), 211–228. doi.org/https://doi.org/10.1016/j.epsl.2005.03.020.
Westerhold, T., Marwan, N., Drury, A.J., Liebrand, D., Agnini, C., Anagnostou, E., Barnet, J.S., Bohaty, S.M., De Vleeschouwer, D., Florindo, F., 2020. An astronomically dated record of Earth's climate and its predictability over the last 66 million years. Science 369(6509), 1383–1387.
Willenbring, J.K., von Blanckenburg, F., 2010. Long-term stability of global erosion rates and weathering during late-Cenozoic cooling. Nature 465(7295), 211–214. doi.org/10.1038/nature09044.
Williams, T.J., Martin, E.E., Sikes, E., Starr, A., Umling, N.E., Glaubke, R., 2021. Neodymium isotope evidence for coupled Southern Ocean circulation and Antarctic climate throughout the last 118,000 years. Quaternary Science Reviews 260, 106915.

Wilson, D.J., Piotrowski, A.M., Galy, A., Banakar, V.K., 2015. Interhemispheric controls on deep ocean circulation and carbon chemistry during the last two glacial cycles. Paleoceanography 30(6), 621–641.

Wilson, D.J., Piotrowski, A.M., Galy, A., Clegg, J.A., 2013. Reactivity of neodymium carriers in deep sea sediments: Implications for boundary exchange and paleoceanography. Geochimica et Cosmochimica Acta 109, 197–221.

Wu, Q., Colin, C., Liu, Z., Thil, F., Dubois-Dauphin, Q., Frank, N., Tachikawa, K., Bordier, L., Douville, E., 2015. Neodymium isotopic composition in foraminifera and authigenic phases of the South China Sea sediments: Implications for the hydrology of the N orth P acific O cean over the past 25 kyr. Geochemistry, Geophysics, Geosystems 16(11), 3883–3904.

Xu, A., Hathorne, E., Laukert, G., Frank, M., 2023. Overlooked riverine contributions of dissolved neodymium and hafnium to the Amazon estuary and oceans. Nature Communications 14(1), 4156.

Yang, Y., Galy, A., Yang, R., Liu, Y., Zhang, W., Ruan, X., Fang, X., Jin, Z., Song, B., Yan, M., 2023. Intense metamorphism-generated radiogenic Sr regulated Cenozoic water Sr isotope evolution on the NE Tibetan Plateau: A perspective on Qilian orogen denudation and Asian eolian transport. Bulletin 135(9-10), 2237–2254.

Yu, Z., Colin, C., Bassinot, F., Wan, S., Bayon, G., 2020. Climate-Driven Weathering Shifts Between Highlands and Floodplains. Geochemistry, Geophysics, Geosystems 21(7), e2020GC008936. doi.org/10.1029/2020gc008936.

Yu, Z., Colin, C., Douville, E., Meynadier, L., Duchamp-Alphonse, S., Sepulcre, S., Wan, S.M., Song, L.N., Wu, Q., Xu, Z.K., Bassinot, F., 2017a. Yttrium and rare earth element partitioning in seawaters from the Bay of Bengal. Geochem Geophy Geosy 18(4), 1388–1403. doi.org/10.1002/2016gc006749.

Yu, Z., Colin, C., Ma, R., Meynadier, L., Wan, S., Wu, Q., Kallel, N., Sepulcre, S., Dapoigny, A., Bassinot, F., 2018. Antarctic Intermediate Water penetration into the Northern Indian Ocean during the last deglaciation. Earth and Planetary Science Letters 500, 67–75. doi.org/https://doi.org/10.1016/j.epsl.2018.08.006.

Yu, Z., Colin, C., Meynadier, L., Douville, E., Dapoigny, A., Reverdin, G., Wu, Q., Wan, S., Song, L., Xu, Z., 2017b. Seasonal variations in dissolved neodymium isotope composition in the Bay of Bengal. Earth and Planetary Science Letters 479, 310–321.

Yu, Z., Colin, C., Wilson, D.J., Bayon, G., Song, Z., Sepulcre, S., Dapoigny, A., Li, Y., Wan, S., 2022. Millennial variability in intermediate ocean circulation and Indian monsoonal weathering inputs during the last deglaciation and Holocene. Geophysical Research Letters 49(21), e2022GL100003.

Zhao, N., Oppo, D.W., Huang, K.F., Howe, J.N.W., Keigwin, L.D., 2019. Glacial–interglacial Nd isotope variability of North Atlantic Deep Water modulated by North American ice sheet. Nature Communications 10(1), 5773.

Zondervan, J.R., Hilton, R.G., Dellinger, M., Clubb, F.J., Roylands, T., Ogrič, M., 2023. Rock organic carbon oxidation CO2 release offsets silicate weathering sink. Nature 623(7986), 329–333.